AD_____

Award Number:
W81XWH-10-1-0598

TITLE:
Role of IKK-alpha in the EGFR Signaling Regulation

PRINCIPAL INVESTIGATOR:
Dr. Chia-Wei Li, PhD

CONTRACTING ORGANIZATION:
The University of Texas M. D. Anderson Cancer Center

Houston, Texas 77030

REPORT DATE:
September 2014

TYPE OF REPORT:
Annual Summary

PREPARED FOR: U.S. Army Medical Research and Materiel Command
Fort Detrick, Maryland 21702-5012

DISTRIBUTION STATEMENT:

■ Approved for public release; distribution unlimited

# REPORT DOCUMENTATION PAGE

*Form Approved*
*OMB No. 0704-0188*



| 1. REPORT DATE *(DD-MM-YYYY)* | 2. REPORT TYPE | 3. DATES COVERED *(From - To)* |
|---|---|---|
| September 2014 | Annual Summary | 15 Aug 2010 - 14 Aug 2014 |

**4. TITLE AND SUBTITLE**
Role of IKK-alpha in EGFR Signaling Regulation

**5a. CONTRACT NUMBER**

**5b. GRANT NUMBER**
W81XWH-10-1-0598

**5c. PROGRAM ELEMENT NUMBER**

**6. AUTHOR(S)**
Chia-Wei Li, PhD

email: cwli@mdandrson.org

**5d. PROJECT NUMBER**

**5e. TASK NUMBER**

**5f. WORK UNIT NUMBER**

**7. PERFORMING ORGANIZATION NAME(S) AND ADDRESS(ES)**

University of Texas M.D. Anderson Cancer Center
Houston, TX 77030

**8. PERFORMING ORGANIZATION REPORT NUMBER**

**9. SPONSORING / MONITORING AGENCY NAME(S) AND ADDRESS(ES)**
U.S. Army Medical Research and Materiel Command
Fort Detrick, Maryland 21702-5012

**10. SPONSOR/MONITOR'S ACRONYM(S)**

**11. SPONSOR/MONITOR'S REPORT NUMBER(S)**

**12. DISTRIBUTION / AVAILABILITY STATEMENT**
Approved for public release; distribution unlimited

**13. SUPPLEMENTARY NOTES**

**14. ABSTRACT**

Overexpression of EGFR is frequently linked to more aggressive tumor behavior, including increased proliferation, metastasis, and therapeutic resistance. Here, we identified a molecular linkage between IKKα and EGFR signaling in breast cancer cells. Inhibition of IKKs activity elevates EGFR tyrosine phosphorylation. In addition, IKKα forms a specific interaction with EGFR in Golgi apparatus and catalyzes EGFR S1026 phosphorylation. We found that EGFR S1026A possess a stronger tumorgenesis phenotype compare with wild type EGFR suggesting a negative regulation of IKKα in EGFR signaling. In agreement with an earlier finding where conditional ablation of IKKα in the mice keratinocytes elevates the autocrine loop of EGFR, our results further provide a potent role of IKKα kinase activity in preservation of EGFR activity.

**15. SUBJECT TERMS**
EGFR signaling, inflammatory kinase, IKKalpha, tumorgenesis, tumor suppressor

| 16. SECURITY CLASSIFICATION OF: | | | 17. LIMITATION OF ABSTRACT | 18. NUMBER OF PAGES | 19a. NAME OF RESPONSIBLE PERSON |
|---|---|---|---|---|---|
| a. REPORT | b. ABSTRACT | c. THIS PAGE | | | 19b. TELEPHONE NUMBER *(include area code)* |
| U | U | U | UU | 69 | USAMRMC |

**Table of Contents**

**Page**

**Title: The role of IKKα in EGFR signaling regulation**

## 1. INTRODUCTION:

A Triple-negative breast cancer (TNBC), which account for approximately 15-20% of breast cancers in the United States, lacks the expression of estrogen receptor (ER) and progesterone receptor (PR) as well as amplification of HER2/neu and is associated with poorer outcome compared with other breast cancer subtypes (*1-3*). TNBC also overlaps with the basal-like breast cancer, which is a subtype of breast cancer classified by genomic signatures identified in the molecular classification, although they are not same (*2, 4*). Unlike ER-positive, PR-positive, or HER2-overexpressing tumors, the lack of well-defined molecular targets and the heterogeneity of the disease pose a challenge for treating TNBC (*1, 3*).

Aberrant activation and overexpression of the epidermal growth factor receptor (EGFR) contribute to aggressive tumor behavior and poor patient prognosis (*5*), and thus drugs that target EGFR are being used to treat many types of cancers. However, they are not as effective for breast cancer, suggesting that other mechanisms (*6, 7*) or biological functions of EGFR that have yet to be discovered may have important roles in breast cancer. Overexpression of EGFR has been frequently observed in TNBC and is associated with poor clinical outcome in TNBC patients (*4, 8*). These findings suggest that further understanding of the role of EGFR is critical for implementing successful anti-EGFR therapy in TNBC.

In this study, we found a major inflammation regulator, IKKα inhibits EGFR activity through a novel signaling pathway in breast cancer cells. IKKα binds to and phosphorylated EGFR at S1026. Inhibits of IKK activity led to hyperphosphorylation of EGFR Y845 and STAT3 Y705. Consistent with an earlier finding that IKKα serves as a tumorsuppressor inducing skin cancer (11), our study provides novel mechanistic insight of IKKα mediated EGFR suppression.

## 2. RESEARCH ACCOMPLISHMENTS BODY

**Part I: Downregulation of IKKα enhances EGFR signaling through STAT3**

In this final year DoD progress report, we have summarized all the progress in a format of manuscript (**please see appendix-1**), which is ready to submit to Cancer Research. During the course of study, we have finished the proposed experiments proving the tumor suppressor function of IKKα is due to the inhibition of EGFR signaling. Briefly, inhibition of IKKα activity by chemical inhibitor or shRNA activates EGFR tyrosine phosphorylation. Similarly, activation of IKKα inhibits EGFR Y845 phosphorylation. In search of IKKα-mediated EGFR suppression, we found IKKα is able to phosphorylate EGFR at S1026 and therefore inhibits the EGFR activity. In the past three years, we have accomplished all proposed experiments. First, we have generate EGFR S1026A functional assay to show that ablation of IKKα phosphorylation on EGFR induces cell proliferation. Second, we have characterized the site-specific antibody and show that phospho-EGFR S1026 is really expressed in vivo. Third, we have generated the transgenic mice with IKKα knockout and EGFR overexpression in mammary gland. These results provide the most in vivo evidence that IKKα is a tumor suppressor in EGFR high expressed cells.

Overall, we have accomplished all proposed experiments and show the most in vivo evidence that EGFR is a tumor suppressor. We appreciate the support by DoD postdoctoral fellowship and expect to submit the work soon.

**Part II: AKT1 inhibits breast cancer EMT by stabilizing Twist1**

The other project we conduct in the DoD fiscal years is to identified the mechanism of AKT1 in EMT inhibition in breast cancer cells. Unlike AKT2, which primarily involved in metastatic dissemination, AKT1 is known to inhibit breast cancer cell migration, invasion and EMT in both transgenic mouse models and cell based studies. In light of several observations all indicate the negative role of AKT1 during metastatic spread, however the underlying mechanisms of the opposing effect by two highly related kinase (AKT1/2) remain largely unknown. In this study, several lines of evidence suggest that AKT1 selectively regulates Twist1 activity and contributes to AKT1-mediated repression of breast cancer metastasis. We found that AKT1 but not AKT2 specifically interacts with Twist1 but not with other EMT mediators both *in vitro* and *in vivo*. Two potential AKT phosphorylation motifs spanning three residues on the Twist1 (S42 and

T121/S123) are required for complete phosphorylation by AKT1. AKT1 negatively regulates Twist1 expression by catalyzing a phosphorylation-dependent ubiquitination on Twist1. Phosphorylation deficient mutant of Twist1, which is resistant to b-TRCP-mediated proteasome degradation, induces a stronger EMT phenotypic change. Downregulation of Twist1 reverts AKT1-mediated EMT repression, suggesting that Twist1 is an authentic regulator governs AKT1-induced EMT repression.

Although an earlier study has indicated the involvement of AKT in Twist1 phosphorylation, here, we provide a more comprehensive study that utilizes a recombinant full-length Twist1 to dissect the contribution of each phosphorylation motif. In their study, PKBb/AKT2 was used to test the phosphorylation on the synthetic peptide to identify S42 as PKBb/AKT2 phosphorylation site. Changing S42 to alanine had modest impact on the anti-apoptosis activity of Twist1. In our study, we found AKT1 but not AKT2 preferentially interacts with Twist1, phosphorylates at three sites, and subsequently alters Twist1 stability. Strikingly, ablation of three AKT1 phosphorylation sites on Twist1 induces a stronger EMT phenotype, which resembles AKT1-mediated EMT repression. In addition, we identified b-TrCP as a novel ubiquitin E3 ligase that targets Twist1 for AKT1-induced degradation. Overall, our observations are novel, timely, and provide new mechanistic insight connecting phosphorylation-dependent ubiquitination of Twist1 to the inhibitory nature of AKT1 in metastatic repression.

Since this work is also related with breast cancer metastasis which is under the theme of the DoD fellowship on breast cancer research. In the appendix-2, we provide complete set of research data for evaluation as the final report.

**Part III: EGFR Associates with and Primes GSK3β for its Inactivation and Mcl-1 upregulation. Supported by DoD funding, the PI also serves as first author of another manuscript related to Triple Negative Breast Cancer (TNBC) treatment.**

In studies with endogenous GSK3β association complex, we identified EGFR as a novel GSK3β-interacting protein, which phosphorylates GSK3β and inhibits GSK3β activation. We revealed that GSK3β's activity is stringently modulated by a previously unknown and reversible modification, ubiquitination through a distinct TRAF6 binding

motif of GSK3β. The essence of PE motif for enhancing GSK3β activity suggested TRAF6-mediated K63 ubiquitinaiton is involved. Furthermore, TRAF6 activates GSK3β activity, thereby affecting GSK3β dependent apoptosis. Altogether, we demonstrate EGFR associates with and phosphorylates GSK3β, which primed inactivation of GSK3β by inhibiting TRAF6-mediated ubiquitination, resulting in Mcl-1 upregulation.

## 3. CONCLUSION

EGFR, as an essential growth and survival factor, plays an important role in cancers of the lung, breast, brain, ovary, skin, and colon. The modification patterns of EGFR are critical for its function and the understanding of these EGFR modifications could help us design the optimal therapeutic strategies for targeting various EGFR-associated cancers and/or non-cancerous diseases. In current study, we identified that EGFR serine phosphorylation as a novel posttranslational modification playing an indispensable role in regulation of EGFR signaling pathways. We identified that IKKα is a serine/theronine kinase responsible for EGFR S1026 phosphorylation. Our data suggest that EGFR S1026 phosphorylation mainly affects its synergic interaction with Src. Similar to other serine/theronine phosphorylation, phosphorylation by IKKα downregulates EGFR signaling and thereby diminishes cell growth and tumorigenesis.

Our results also provide the first mechanistic evidence of how IKKα could serve as a tumor suppressor. In the past three years, we have focused targeting EGFR signaling in triple negative breast cancer cells. With DoD's support, we have addressed important biology question in human breast cancer cells and hoping to provide useful treatment for breast cancer patients.

## 4. KEY RESEARCH ACCOMPLISHMENTS: 2013-2014

a) Manuscript preparation of the role of IKKα in EGFR signaling regulation.

b) Submission of AKT1 mediated EMT suppression.

## 5. REPORTABLE OUTCOMES 2013

**Li CW**, Xia W, Huo L, Lim SO, Wu Y, Hsu JL, Chao CH, Yamaguchi H, Yang NK, Ding Q, Wang Y, Lai YJ, Labaff AM, Wu TJ, Lin BR, Yang MH, Hortobagyi GN, Hung MC. (2012) *Epithelial-Mesenchymal Transition Induced by TNF-α Requires NF-κB-Mediated Transcriptional Upregulation of Twist1*.**Cancer Research** 72(5): 1290-1300

Wang Y, Ding Q, Yen CJ, Xia W, Izzo JG, Lang JY, **Li CW**, Hsu JL, Miller SA, Wang X, Lee DF, Hsu JM, Huo L, Labaff AM, Liu D, Huang TH, Lai CC, Tsai FJ, Chang WC, Chen CH, Wu TT, Buttar NS, Wang KK, Wu Y, Wang H, Ajani J, Hung MC. (2012) *The crosstalk of mTOR/S6K1 and Hedgehog pathways.* **Cancer Cell**. 20;21(3):374-87.

**Li CW**, Lai CC, He X, Chao CH, Sun HL, Yamaguchi H, Xia W, Wang Y, Chou CK, Hsu JM, Lee DF, Ding Q, Wang H, Labaff A, Hung MC. (2014) Phosphorylation of Twist1 at multiple sites by AKT1 modulating EMT in breast cancer cells. *In submission*

**Li CW**, Ding Q, Xia W, Lai CC, Wang Y, Huo L, Li HJ, Lamothe B, Campos AD, Hur L, Lai YJ, Darnay BG and Hung MC. (2014) The role of IKKα in EGFR signaling regulation. *In preparation*

## 6. REFERENCE:


1. Citri, A., and Yarden, Y. (2006) *Nature reviews. Molecular cell biology* **7**, 505-516
2. Yarden, Y. (2001) *Eur J Cancer* **37 Suppl 4**, S3-8
3. Yarden, Y., and Sliwkowski, M. X. (2001) *Nature reviews. Molecular cell biology* **2**, 127-137
4. Herbst, R. S., Fukuoka, M., and Baselga, J. (2004) *Nature reviews. Cancer* **4**, 956-965
5. Sharma, S. V., Bell, D. W., Settleman, J., and Haber, D. A. (2007) *Nature reviews. Cancer* **7**, 169-181
6. Sordella, R., Bell, D. W., Haber, D. A., and Settleman, J. (2004) *Science* **305**, 1163-

1167

7. Nyati, M. K., Morgan, M. A., Feng, F. Y., and Lawrence, T. S. (2006) *Nature reviews. Cancer* **6**, 876-885
8. Zhang, X., Gureasko, J., Shen, K., Cole, P. A., and Kuriyan, J. (2006) *Cell* **125**, 1137-1149

## 7. APPENDICES:

A. manuscript of IKKα mediated EGFR signaling downregulation

B. manuscript of AKT1 mediated breast EMT inhibition

# IKKalpha negatively regulates EGFR signaling by interfering Src activation

Chia-Wei Li[1], Longfei Huo[1], Seung-Oe Lim[1], Jennifer L. Hsu[1,6,7], Jung-Mao Hsu[1], Weiya Xia[1], Chien-Chen Lai[5], Hirohito Yamaguchi[1], Yan Wang[1], Yun-Ju Lai[3], Adam M. LaBaff[1,4], Qingqing Ding[1], How-Wen Ko[1,4,9], Fuu-Jen Tsai[6], Chang-Hai Tsai[6], Gabriel N. Hortobagyi[3], and Mien-Chie Hung[1,4,6,7,*]

[1]Department of Molecular and Cellular Oncology, [2]Department of Experimental Therapeutics, and [3]Department of Breast Medical Oncology, The University of Texas MD Anderson Cancer Center, Houston, TX 77030, USA

[4]Graduate School of Biomedical Sciences, The University of Texas Health Science Center, Houston, TX 77030, USA

[5]China Medical University Hospital, Taichung 404, Taiwan

[6]Center for Molecular Medicine and Graduate Institute of Cancer Biology, China Medical University and Hospital, Taichung 404, Taiwan

[7]Department of Biotechnology, Asia University, Taichung 413, Taiwan

[8]State Key Laboratory of Oncogenes and Related Genes, Shanghai Cancer Institute, Shanghai 200032, China

[9]Department of Chest Medicine, Chang Gung Memorial Hospital, Taipei, Chang Gung University College of Medicine, Taoyuan, Taiwan

*Correspondence: Mien-Chie Hung, Department of Molecular and Cellular Oncology, Unit 108, The University of Texas MD Anderson Cancer Center, 1515 Holcombe Blvd., Houston, TX 77030. Phone: (713) 792-3668. Fax: (713) 794-3270. E-mail: mhung@mdanderson.org

**Running Title:** IKKα suppresses EGFR signaling via Src-mediated EGFR Y845 phosphorylation

**Keywords:** IKKα, EGFR, Src, Y845 phosphorylation, STAT3, tumor suppressor

**Summary**

Epidermal Growth Factor Receptor (EGFR) belongs to the HER2 family of Receptor Tyrosine Kinases (RTKs). Overexpression of EGFR is frequently linked to more aggressive tumor behavior, including increased proliferation, metastasis, and therapeutic resistance. In particular, patients harboring breast tumors with high EGFR survived poorly compared with those no or low levels. Thus, EGFR has been considered as an excellent target of anticancer therapy for breast cancer. In this study, we identified that EGFR serine phosphorylation as a novel posttranslational modification playing an indispensable role in regulation of EGFR signaling cascades. We found that IKKα directly binds to and phosphorylates EGFR at Serine 1026. Substitution of Serine 1026 to Alanine (S1026A) enhances Src mediated EGFR Y845 and STAT3 activity, suggesting a negative role of IKKα in regulating EGFR and Src synergism. An in-depth analysis of this novel axis, IKKα/EGFR/STAT3, reveals that CCL2 is a specific target for STAT3 regulation. In agree with serine/threonine phosphorylation-mediated RTK repression, we herein identified IKKα downregulates EGFR signaling and thereby diminish cell growth and tumorigenesis in breast cancer cells.

**Introduction:**

Breast cancer is one of the most common types of cancer in women in the United States. Despite advances in imaging and treatment, more than 40,000 women die of this disease each year. Through extensive studies, it has been shown that breast cancer progression is caused by deregulation of signaling pathways (1). For example, 25% of patients with breast cancer have amplification and/or overexpression of receptor tyrosine kinase (RTK). Epidermal Growth Factor Receptor (EGFR) belongs to the ErbB family of RTKs. Overexpression of EGFR is frequently linked to more aggressive tumor behavior, including increased proliferation, metastasis, and therapeutic resistance (2). In particular, breast cancer patients that contain high EGFR expression survived poorly compared to those with little or no expression. Thus, EGFR has been considered as an excellent target of anticancer therapy (3) (2).

Upon Ligand binding, EGFR dimerizes, autophosphorylates, and triggers a myriad of downstream signaling, such as the activation of phosphoinositide 3 kinase-protein kinase B (PI3K-PKB/AKT), mitogen-activated protein kinase (MAPK), Jak/the signal transducers and activators of transcription (STAT), Rho family GTPase (VAV2), and Phospholipase C (PLCγ) (4). These signaling activities regulate cell proliferation, mobility, and differentiation in many different cell types (5). To date, tyrosine phosphorylation of EGFR is well characterized and most of them respond to ligand stimulation. Y845 (Tyr845) phosphorylation by c-Src is implicated in stabilizing the activation loop, maintaining the enzyme activity and providing a binding surface for the STAT3 (6,7). Y992 is a direct binding site for the PLCγ SH2 domain, resulting in activation of PLCγ-mediated downstream signaling (8). Y1045 phosphorylation creates a major docking site for c-Cbl, an ubiquitin E3 ligase, leads to receptor ubiquitination and degradation. Y1068 phosphorylation recruits Grb2 (9) whereas, phospho-tyrosine 1148 and 1173 provide a docking site for SHC binding (7). Except for all these extensively studies, serine and threonine phosphorylation of EGFR is less understood, and they often relates to negatively regulation of EGFR (10). For example, S1046 and S1047 phosphorylation by CaM kinase II attenuates EGFR kinase activity, and mutation of either of them upregulates EGFR tyrosine kinase activity (11). T669 phosphorylation by $P38^{MAPK}$ (12) or Erk (13) downregulates receptor signaling involving in cisplatin induced chemoresistance. Most recently, AKT-mediated EGFR S229 phosphorylation is required for EGFR nuclear translocation (14).

Signal transducers and activators of transcription 3 (STAT3) is a key regulator in

response to cytokines and growth factor receptor (15). STAT3 possesses oncogenic potential and is constitutively activated in many types of cancer including 30-60% of breast cancer (16). This transcription factor is activated by Y705 phosphorylation, and in turn triggers its dimerization, nuclear translocation and DNA binding. The association between EGFR and STAT3 appears both in cytoplasm and nucleus (16), their coexpression leads to enhance the metastatic potential of breast cancer cells (17).

IKKα is a component of the classic IKK complex, which is composed of three subunits: two catalytic kinases (IKKα and IKKβ) and a regulatory scaffold partner (IKKγ). Upon stimulation by either TNFα or IL-1β, activated IKKα/β phosphorylates the NFκB inhibitor IκBα and disrupts the nuclear retention of NFκB. In fact, IKKα does more than simply facilitates IκBα degradation for NFκB activation. In the non-canonical pathway, IKKα is also known to phosphorylate substrates to promote cell survival (18). Despite all these reports reveal the oncogenic potentials of IKKα (19), till recently, deletion of IKKα in keratinocytes causes skin defects in conditional knockout mice (20). For the first time, this finding suggests the role of IKKα acts as a tumor suppressor in preventing skin cancer. Additionally, MEF cells lacking IKKα show nuclear cyclin D1 overexpression further consolidates the tumor suppressor role of IKKα (21). Later on, the antiproliferation activity of IKKα is found to be capable of inhibiting TGFβ signaling (22). To identify the underlying mechanism of IKKα-mediated tumor suppression, we herein demonstrate a kinase dependent tumor suppressor function of IKKα in breast cancer cells. Inhibition of IKKα activity through chemical inhibitor or shRNA enhances EGFR Y845 phosphorylation and subsequently activates its downstream target, STAT3. Interestingly, EGFR S1026A, which failed to be phosphorylated by IKKα, showed higher activity of EGFR pY845 and p-STAT3 compared to EGFR wild-type cells. In agree with earlier findings, our result identify a novel molecular signaling dissecting IKKα-mediated tumor suppressor function in breast cancer cells.

## Results

### IKKα inhibits EGFR signaling is kinase dependent

To understand the underlying mechanism of EGFR regulation, various inhibitors were selected and tested their effect on EGFR tyrosine phosphorylation using an anti phospho-tyrosine

antibody (4G10) (Fig. 1A). Among all tested inhibitors, Bay 11-7082 (Calbiochem), an IKK kinase inhibitor, unexpectedly enhance EGFR tyrosine phosphorylation in the presence of 25 ng/ml EGF treatment (Fig. 1B). To determine the tyrosine residue might respond to the EGFR activation, six anti-phospho-tyrosine antibodies of EGFR (pTyr845, pTyr992, pTyr1068, pTyr1086, pTyr1148, and pTyr1173) were also examined. We found that Bay 11-7082 drastically enhances pTyr845 activation, whereas others remain virtually no activation in MDA-MB-468 cells (Fig. 1D). We also examine the activation of EGFR downstream targets PLCγ1 (pTyr783), VAV2 (pTyr172), STAT3 (pTyr705), AKT (pSer470), and ERK (pTyr204) in the presence of Bay 11-7082 treatment. Surprisingly, inhibition of IKK results in specific activation of EGFR Tyr845 and STAT3 Tyr705 (Fig. 1C). To exclude the off-target effect caused by chemical inhibitors, we used siRNA to knockdown IKKα and IKKβ expression. Consistent with our earlier finding, downregulation of IKKα elevates EGFR Tyr845 phosphorylation and p-STAT3 status, supporting the notion that EGFR activity is negatively regulated by IKKα. In addition, MEF cells with IKKα deficiency show elevated EGFR Y845 phosphorylation and STAT3 activation (Fig. S1A). Stably expressing IKKα inhibits EGFR Y845 and STAT3 status (Fig. S1B). Consistence with an earlier finding, the kinase activity IKKα is important for EGFR activity.

**IKKα binds to EGFR and inhibits EGF induced Src and EGFR interaction**

Our finding that inhibition of IKK activates EGFR signaling prompted us to investigate the mechanism by which IKK mediated downregulation of EGFR. Since the IKK complexes are the upstream molecules responsible for the regulation of NFκB activity, we investigated whether the regulation of EGFR by NFκB pathway via IKK complex (IKKα, IKKβ, and IKKγ). To do so, HEK 293 cells were transiently transfected with EGFR together with Flag-IKKα, IKKβ, and IKKγ. Coimmunoprecipitation (Co-IP) showed that IKKα but not IKKβ or IKKγ physically associates with EGFR (Fig. 2A). Similar results were confirmed using a reverse IP (Fig. 2B). The specific interaction between IKKα and EGFR was also observed at endogenous level in MDA-MB-468 cells using specific antibodies against IKKα and EGFR (Fig. S2A). To test the direct physical interaction, an *in vitro* GST pull down assay was conducted and identified EGFR preferentially interacts with IKKα N-terminal domain (Fig. 2C). In addition to their physical

interaction, cellular fractionation assay reveals that both IKKα and EGFR colocalized in the Golgi apparatus upon EGF stimulation (Fig. S2B). To understand the underlying mechanism by which the inhibition of IKKα results in EGFR hyperactivation, we noted that EGFR Y845 is directly regulated by Src. We therefore tested whether IKKα affects the binding between EGFR and Src to attenuate EGFR signaling. We found that EGF-induced EGFR/Src interaction was transient as it peaked within a few minutes and disappeared after 1 hr of EGF stimulation. Inhibition of IKKα using Bay 11-7082 enhances EGFR and Src physical interaction (Fig. 2D). In addition, stably expression of IKKα in MDA-MB-468 cells suppresses Src activity by preventing Src and EGFR association (Fig. 2E). To recapitulate EGFR and Src interaction in the real time, a DuoLink assay was performed and examined under confocal microscopy. MDA-MB-468 cells stained with either EGFR or Src antibody showed no signal (data not shown). Co-staining with both EGFR and Src antibodies significantly amplified the signal of Texas red reporter (Fig. 2F, upper panel) suggesting that they are in close proximity. Similarly, stably expressing IKKα reduces EGFR and Src interaction (Fig. 2F, lower panel). Altogether, these results suggest that IKKα interferes with EGFR and Src synergetic activation resulting in EGFR Y845 inactivation.

**IKKα does not affect EGFR ubiquitionation and degradation**

Phosphorylation of EGFR at Y1045 triggers Cbl-mediated ubiquitination and induces EGFR ubiquitination and proteasome-dependent protein degradation (23-25). It is therefore of interest to know whether IKKα affects EGFR signaling pathway by modulating protein turnover. To do this, we measure EGF mediated EGFR ubiquitination in both inhibitor and knockdown experiment. As shown in the Figure S3D, manipulating of IKKα does not influence EGFR ubiquitination. In addition, overexpression of IKKα failed to induce EGFR ubiquitination (Fig. S3E and S3F). Consistent with our hypothesis, IKKα specifically affects EGFR Y845/Src interaction but not EGFR Y1045/Cbl mediated protein turnover.

**IKKα phosphorylates EGFR at S1026**

Given the physical association between IKKα and EGFR, we examined whether EGFR is a physiological substrate of IKKα. To test this hypothesis, EGFR together with IKKα, nIKKα (dominant negative), K144M (kinase dead) and IKKβ were overexpressed in HEK 293 cells and

subjected to IP of EGFR. We found that IKKα catalyzes EGFR serine phosphorylation using an anti phospho-serine antibody (Fig. 3A) and treatment with Bay 11-7082 abrogates this phosphorylation (Fig. S3A). Since IKKα/β activates one another in the transient transfection system, we utilized an *in vitro* kinase assay in the following experiment. We found that the EGFR C-terminal domain (CR, aa 978-1211) was strongly phosphorylated by IKKα, whereas other domains (JM, aa 650-718 and KD, aa 718-978) were not (Fig. S3B and S3C). Although S669A and S976A of EGFR complete abolishes P38 $^{MAPK}$ phosphorylation (12) (Fig. S3D), they do not affect IKKα-mediated EGFR phosphorylation. To pinpoint the IKKα-mediated EGFR phosphorylation site, mass spectrometry analysis of *in vitro* kinase assay reveals that EGFR Ser1026 is phosphorylated by IKKα (Fig. 3B). Mutation of Ser residue into Ala (S1026A) but not other known phosphorylation sites on the EGFR-CR abolishes the phosphorylation by IKKα (Fig. 3C), suggesting that IKKα directly phosphorylates EGFR at S1026.

Because EGFR S1026 phosphorylation remains unidentified, we noted that EGFR S1026 is highly conserved across species (Fig. 3D). To recapitulate IKKα mediated EGFR S1026 phosphorylation, we purified and analyzed the phospho-EGFR S1026 antibody. As shown in Figure 3E, IKKα induces a nice phosphorylation of EGFR in overexpression system. Mutation of Ser 1026 to Ala (S1026A) abolishes IKKα mediated EGFR phosphorylation. We next examined the membrane localization of EGFR S1026 phosphorylation in MDA-MB-468 cells. Using confocal microscopy, endogenous EGFR and p-EGFR S1026 expression shows a non-overlapped membrane colocalization (Fig. 3F). To test S1026 phosphorylation at physiological conditions, MEF cells were treated with RANKL at indicated time points. Ablation of IKKα abrogates RANKL mediated EGFR S1026 phosphorylation (Fig. S3F). To identify a physiological correlation, we investigated IKKα and p-EGFR S1026 expression in 13 human breast cancer cell lines. A positive correlation between IKKα and p-EGFR S1026 expression (correlation coefficient $r=0.63$, $p<0.05$) was found, suggesting that high IKKα promotes EGFR phosphorylation in breast cancer cells (Fig. 3G).

**Phosphorylation of S1026 inhibits EGFR and Src binding to attenuate EGFR signaling**

The biological activity of IKKα-mediated EGFR S1026 phosphorylation was vigorously achieved. To do this, we established EGFR stable transfectants with EV (empty vector), EGFR

wild type, EGFR DN (dominant negative, D837A), a well-known patient mutation (L858R) and S1026A in NIH3T3, CHO and MCF7 breast cancer cell lines, in which the basal level of EGFR is low. The functional analysis of EGFR utilizing these cells for various purposes has been well established (26). Therefore, these cell lines served as good recipients for establishing stable transfectants of EGFR and its variants. To create EGFR stable clones, we utilized replication incompetent retroviruses produced from pBABE-EGFR vectors (27). Cells were then selected using 2 μg/μl puromycin for 10 days to remove low- or non-infected cells. To rule out the possibility that protein conformational misfolding may occur by amino acid substitution, we analyzed the membrane association of EGFR (Fig. 4A) and their ligand binding ability (data not shown). As shown in the Figure 4A, the distribution of membrane bound EGFR are similar in all stable clones compared to the cells infected with empty vector, suggesting that mutation of EGFR does not influence its cellular property. To investigate the activation of EGFR signaling, stable transfectants were serum-starved overnight and treated with 25 ng/ml for various time points. Indeed, EGFR WT activated a good induction of p-STAT3, p-AKT, or p-Erk in response to EGF treatment, whereas EGFR DN failed to do so. Consistent with our hypothesis, EGFR S1026A showed a higher activation of Tyr845 and p-STAT3 with similar degree to that of EGFR L858R. In fact, EGFR S1026A mediated hyperactivation is specific, because p-AKT and p-Erk status did not change compared with EGFR WT (Fig. 4B and S4A). To test the biological behavior of EGFR S1026A, a 3-(4,5-dimethylthiazol-2-yl)-2,5-diphenyltetrazolium bromide (MTT) colorimetric assays was performed. We observed that MCF7-EGFR (S1026A) cells grow more quickly than MCF7-EGFR (WT) cells, whereas MCF7-EGFR DN showed a reduced growth (Fig. 4C). To test whether the fast proliferation of EGFR S1026A account for tumorigenesis, we performed clonogenic assay and BrdU analysis to observe *in vitro* cell proliferation rate using MCF7 stable cell clones (Fig. 4C and 4D). In addition, we investigated whether EGFR S1026A could support breast cancer MCF7 cell to grow tumor *in vivo* using orthotopic animal model. MCF7 stable clones expressing either EV, EGFR WT, EGFR DN, or EGFR S1026A were injected into mammary fat pads of nude mice and tumor sizes were measured at indicated time points. As shown in Figure 4F and 4G, EGFR S1026A stimulates MCF7 cells to grow tumor in compare with EGFR WT. Together, our *in vitro* and *in vivo* results support that EGFR S1026 phosphorylation plays an essential role in regulating cell growth, DNA synthesis, and tumorigenesis.

**IKKα functions as a tumor suppressor in breast cancer cells**

To investigate IKKα-mediated STAT3 downregulation via EGFR, a luciferase reporter assay was performed. We found a STAT3 reporter, Lye6-Luc, responds to STAT3 CA (constitutive activate)-induced stimulation in HeLa cells, whereas overexpression of STAT3 DN fails to do so (data not shown). Moreover, co-expression of IKKα, but not IKKβ or IKKγ, significantly reduces STAT3 CA mediated reporter activity (Fig. 5A). Similar experiment were performed in HeLa-shCTRL and HeLa-shEGFR cells, we found that IKKα mediated STAT3 repression requires EGFR (Fig. 5B). To identify the potential STAT3 downstream target that regulated by IKKα, we examine gene expression profile of IKKα (NCBI gene ID: Chuk) using public data set generated from 917 cancer cell line (CCLE) (28). We compared the expression profile of IKKα and 60 STAT3 downstream targets in breast cancer cells (29). Among then, 12 genes show negatively correlated with IKKα expression using CCLE. nonsupervised hierarchical clustering analysis was performed based on Erbb2, ERα (ESR1), PR (PgR) and EMT profile. Strikingly, the gene list was able to distinguish basal-like from luminal type breast cancer cells with high accuracy (90% properly segregated) (Fig. 5C). To pinpoint the exact STAT3 downstream being regulated by IKKα/EGFR signaling, the 12 genes expression profile was determined in EGFR stable clone and IKKα MEF cells by real-time PCR. Interestingly CCL2 was significantly increased in both EGFR S1026A cells and IKKα -/- cells. These results indicate that CCL2 is the specific STAT3 target downregulated by IKKα through EGFR.

We next asked if clinical distinct group of patient samples also shared the differential expression pattern of IKKα. First, we analyzed IKKα genes expression from Netherlands Cancer Institute (NKI) data set, *n*=295 (30). To do this, patients in the NKI cohort were first dichotomized according to expression levels of IKKα. As expected, two groups of breast cancer patients showed a significant difference in recurrence-free survival (RFS; Figure 5D). When the patients were dichotomized according to expression level of IKKα, RFSs of patients with higher expression of IKKα were significantly better than that of those with lower expression of IKKα (Fig. 5D and 5E).

**IKKα–mediated STAT3 activation requires EGFR**

Consistently, IKKα deficient MEF cells specifically upregulated EGF-induced Tyr 845 phosphorylation and p-STAT3 status (Fig. 6A). In addition, stably overexpression of IKKα KD (Kinase dead) and IKKα CA (constitutive activated) in MDA-MB-468 cells showed lower EGFR p-Y845 and p-STAT3 status (Fig. 6B). These results indicate that IKKα inhibits EGFR activity by suppressing EGFR Y845 phosphorylation and STAT3 activity. To investigate IKKa mediated STAT3 downregulation via EGFR, we use a luciferase reporter construct, Lye6-Luc in responded to STAT3 CA stimulation in HeLa cells (Fig. 3C). In contrast, overexpression of STAT3 DN fails to do so (data now shown). Moreover, co-expression of IKKα, but not IKKβ or IKKγ, significantly reduces STAT3 mediated reporter activity. Similar experiment were performed in HeLa- shCTRL and HeLa-shEGFR cells,

**Discussion**

To date, both EGFR and HER2 have been targeted for the development of anti-cancer therapies and many anti-EGFR/HER2 therapies and have proven with promising pre-clinical and clinical outcomes compare to conventional therapy. So far, however, drugs aimed at directly inhibiting EGFR/HER2 activity have met with their limitations in the cancer clinic. For example, the somatic mutations of EGFR have been identified with more or less sensitivity to gefitinib/erlotinib in non-small cell lung cancer (NSCLC) patients (31,32). A review of 3016 cases from the literature indicated that EGFR mutations are associated with gender, races, non-smokers, and histological subtypes (33), which improves pharmacogenetics selection of more appropriate therapies in NSCLC patients. In this regard, identifying the molecular mechanism and post-translational regulation of EGFR may add a novel therapeutic impact to improve anti-EGFR therapeutic efficacy in the clinic use. Given the malignant nature of EGFR overexpression in breast cancer remains elusive and drug resistance remains a major challenge for cancer therapy, the current study is aimed at elucidating new regulatory mechanism of EGFR in breast cancer malignancy.

Unlike the tyrosine phosphorylation and ubiquitination (34), neddylation (35), methylation (26), acetylation (36) (37) and serine/threonine phosphorylation (19) of EGFR are much less characterized and their molecular functions remain largely unknown. To date, several studies indicated EGFR serine/threonine phosphorylation suppresses its functionality (13) (14).

Overexpression of TAK1 inhibits EGFR tyrosine phosphorylation (14). Mutation of EGFR phospho-serine residue elevates its EGFR tyrosine phosphorylation (13). In this study, we report a novel serine phosphorylation of EGFR and its upstream kinase. Similar to most serine phosphorylation, S1026 phosphorylation also plays a negative role in EGFR signaling. Since EGFR Ser1026 phosphorylation occurs both *in vitro* and *in vivo* (Fig. 3), no specific functional analysis has yet been addressed. Given the inhibitory nature of EGFR remains unknown, characterization of this novel post-translational modification on EGFR would likely benefit the field of cancer biology.

The phosphorylated EGFR provides docking sites for binding downstream adaptor proteins and thereafter activates several downstream signaling pathways. Several autophosphorylation tyrosine residues in the intracellular domain of EGFR such as Y992, 1068, 1086, and 1173 have been well characterized. They provide docking sites for adaptor proteins such as Shc, Grb2, or Gab to activate PI3K/Akt and Ras/MAPK signaling pathways (38)(1,9,10). On the other hand, Src-induced transphosphorylation of Y845 on EGFR provides docking site to recruit Stat3/5 and subsequently activated STAT3 and/or STAT5 through the formation of homo- or hetero-dimers. The dimerized STAT3 or STAT5 translocates into the nucleus, binds to its cogent DNA to regulate cell proliferation, differentiation, cell cycle, and migration. Thus far, several tumor suppressors are known to inhibit cell growth by inhibiting EGFR and Src interaction. For example, Csk-binding protein (CBP) inhibits cellular transformation by interfering EGFR/Src activation (39). … Similarly, IKKα affect protein location confirmation by interfering EGFR/Src interaction. This result further explains the inhibition of IKKα elevates Y845 and STAT3.

The link between inflammation and tumor progression has been suspected for about two hundred years, and accumulating evidence supports a tumor-promoting role of inflammation. The proinflammatory cytokines and chemokines produced in the tumor microenvironment, such as TNFα, IL-1, IL-6, and IL-8, enhance cell proliferation, cell survival, cell migration, and tumor angiogenesis, thereby promoting tumor development (40). For example, we have previous shown that IKKβ-induced TSC1 phosphorylation inhibits its association with GTPase-activating protein (TSC2), alters mTOR activity, allows VEGF-A expression, and promotes tumorigenesis (10). IKKα also phosphorylates CBP to changes its binding affinity from P53 to NFκB (41). Recently, we found IKKα phosphorylates FOXA2. Despite these results all indicate tumor-promoting

function of IKKα. However, a recent study show that deletion of IKKα in keratinocytes cause skin defects in a conditional knockout mice, suggesting that the tumor suppressor activity of IKKα in preventing skin cancer (20). Consistent with this observation, this study identify a novel molecular mechanism to link inflammation to breast cancer regression. First, we prove the IKKα-mediated tumor suppression is kinase dependent. Inhibition of IKK kinase activity enhances EGFR signaling. Secondly, we identify a novel serine phosphorylation of EGFR. Given the serine/threonine phosphorylation negatively regulates EGFR's activity (13) (14), we herein provide another rationale for IKKα mediated EGFR suppression. Thirdly, IKKα inhibits Src mediated EGFR Y845 phosphorylation. Lastly, IKKα expression in CCLE dataset shows negative correlation with TNBC phenotype suggesting that IKKα is negatively correlated with STAT3 downstream target. Altogether, we found a major inflammation regulator, IKKα, inhibits EGFR activity through a novel signaling pathway in breast cancer cells. IKKα binds to and phosphorylated EGFR at S1026. Inhibits of IKK activity led to hyperphosphorylation of EGFR Y845 and STAT3 Y705. Consistent with an earlier finding that IKKα serves as a tumor suppressor (20), our study provides novel mechanistic insight of IKKα mediated EGFR suppression.

**Experimental Procedures**

*Plasmids*. pCMV5-HA-IKKα WT, IKKα SSEE, IKKα KA and pcDNA6-EGFR were described previously (26) (10). pBABE-EGFR WT, DN, and L858R were purchased from Addgene (27). EGFR S1026A were generated with using a Quick Change site-directed mutagenesis kit (Stratagene, La Jolla, CA). pCMV-Flag-IKKβ, pCMV-Flag-IKKγ, pCMV-Flag-IKKε and the STAT3-luciferase reporter were described previously (42). All constructs were confirmed by enzyme digestion and DNA sequencing. Detailed information is available upon request.

*Coimmunoprecipitation and Western blot*- Co-immunoprecipitation was conducted according to the standard procedure using protein A-agarose beads (Santa Cruz, Delaware, CA). The cells were lysed in cell lysis buffer (0.4 M NaCl, 0.2 mM EGTA, 10 % glycerol, 0.5 % Nonidet P-40, 1 mM DTT and 1x protease inhibitor), and cell extracts were pre-cleared by incubating with protein A-agarose beads for 1 h at room temperature. A total of 1mg of cell lysates was used for

immunoprecipitation with 1μg of corresponding antibody. The bound proteins were resolved on SDS-polyacrylamide gel and Western blot was performed as described in (10).

*Flow cytometry*. 1x105 MCF7 cells or stable clones were incubated with either FITC-labeled EGF or FITC-labeled antibody against EGFR for 5 min or 30 min, respectively. The cells were then fixed with pre-cold methanol and analyzed by flow cytometry at MD Anderson Core Facilities.

*Tumorigenesis assay.* Orthotropic breast cancer mouse model analyzing tumorigenesis was conducted as previous described (26). A total of 80 mice carrying MCF7-EV, MCF7-EGFR, EGFR DN and EGFR S1026A were established via mammary fat pad injection to measure the impact of cell proliferation *in vivo*.

**Acknowledgments**

We would like to thank xxx at Scientific Publication at MD Anderson Cancer Center for editing the manuscript. This work was partially supported by the National Institutes of Health grants (R01 CA109311 and PO1 CA099031), Kadoorie Charitable Foundations, Patel Memorial Breast Cancer Endowment Fund and National Breast Cancer Foundation, Inc., National Institutes of Health Breast Cancer SPORE (CA116199), Cancer Center Support Grant (CA16672), Breast Cancer Research Foundation grant (to M.-C.H. and G.N.H.), Department of Health Cancer Research Center of Excellence (DOH101-TD-C-111-005 to M.-C.H; Taiwan), and a postdoctoral fellowship from the U.S. Army Breast Cancer Research Program (W81XXWH-10-1-0598 to C.-W.L.)

**Figure and legends**

**Figure 1. Inhibition of IKK activity enhances EGFR signaling**

(A) Inhibition of IKK elevates EGFR tyrosine phosphorylation. MDA-MB-468 cells were pretreated with Bay 11-7082 and LY294002 for 45 mins. Total tyrosine phosphorylation of EGFR was IP and examined using anti-Tyrosine phosphorylation antibody (4G10). (B) Inhibition of IKK enhances EGFR signaling. Similar experiment procedure was performed in

MDA-MB-468 cells with various protein kinase inhibitors. As indicated, inhibition of IKK activity enhances EGFR tyrosine phosphorylation. (C) Inhibition of IKK activates EGFR Tyr845/p-STAT3 signaling axis. MDA-MB-468 cells were pretreated with BAY 11-7082 prior to 30 ng/μl EGF treatments for various time points. EGFR tyrosine phosphorylation and its downstream targets expression were examined. (D) Downregulation of IKKα activates EGFR Tyr845/p-STAT3 signaling axis. (E) Overexpression of IKKα inhibits EGFR signaling.

**Figure 2. IKKα interacts with EGFR abrogates EGFR/Src interaction**

(A) IKKα specifically interacts with EGFR. HEK 293 cells were transiently transfected with indicated plasmids. IP (A) and reverse IP (B) were performed using anti-EGFR or anti-Flag antibodies. Protein interaction was determined by western blot. (C) EGFR preferentially interacts with IKKα at its N-terminal region. Two fragments of IKKα and IKKβ were fused with GST and purified from *E.coli* BL21 cells. $^{35}$S-methioine labeled EGFR was incubated with GST proteins and subject to pull down analysis. (D) Inhibition of IKKα enhances EGF-induced EGFR-Src association. MDA-MB-468 cells were pretreated with Bay 11-7082. EGFR and Src interaction were analyzed using IP and Western blot. (E) IKKα interferes EGF induced EGFR-Src association. MDA-MB-468 cells stably expressing empty vector (pBABE) or IKKα were subject for IP/Western analysis. (F) Dual link analysis showing IKKα inhibits EGFR/Src interaction. Arrow indicated the foci formation.

**Figure 3. IKKα phosphorylates EGFR at S1026 *in vitro* and *in vivo***

(A) IKKα phosphorylates EGFR in cells. HEK 293T cells with indicated plasmids were immunoprecipitated with monoclonal anti-EGFR antibody. Approximately 5% of the cell extract used from each immunoprecipitation reaction was served as input. The total amount of immunoprecipitates (IP) was analyzed by Western blot with anti-phospho Ser/Thr antibodies to detect the *in vivo* phosphorylation. (B) Identification of Ser 1026 phosphorylation *in vitro* by Mass spectrometry. (C) Mutation of EGFR Ser 1026 to Ala abolishes IKKα mediated EGFR phosphorylation. In vitro kinase asssy was performed using recombinant IKKα and GST-EGFR variants. (D) Conservation of EGFR S1026 among different species. Amino acid sequence alignment of EGFR among different species. (E) IKKα phosphorylates EGFR at S1026. HEK

293 cells were transfected with indicated plasmids. EGFR was immunoprecipitated and western blotted with p-EGFR S1026 antibody. (F) Membrane non-overlapped localization of EGFR and pS1026. MDA-MB-468 cells were fixed and subject to immunofluorescence staining using mouse anti-EGFR (AB13) and rabbit anti-p-EGFR S1026 antibody. (G)

**Figure 4. EGFR S0126A exhibits hyperactivation in p-EGFR Y845 and p-STAT3.**

(A) NIH3T3 stable clones carry various EGFR variants were subjected to FACS analysis to identified their membrane EGFR localization. As wild type NIH3T3 cells harbor low EGFR expression, the EGFR variants stable clones showed similar expression and localization. (B) EGFR S1026A shows hyperactivation of p-EGFR Y845 and p-STAT3 Y705. EGFR stable clone were serum starved for overnight and treated with 30 ng/μl EGF for indicated time points and analyzed by western blot. (C) EGFR S1026A induces higher DNA synthesis rate. MCF7 stable transfectants were seeded in 6-well culture plates and cultured to reach 90% confluence. The cells then were serum-starved and treated with Bromodeoxyuridine (BrdU) for 18 hr prior to assay. (D) Colongenic assay showing EGFR S1026A bears higher tumorigenesis ability. (E) MCF7 stable clone cells were inoculated into mammary fat pads of nude mice. The tumor size was measured and statistically analyzed by student's t-Test in (F).

**Figure 5. IKKα negative regulated EGFR signaling**

(A) IKKα inhibits STAT3 transcriptional activity. HEK-293 cells were transfected with the lye6-Luc together with indicated plasmids. The luciferase activity was measured and normalized according to *Renilla* luciferase activity. (B) EGFR is required for IKKα mediated STAT3 inhibition. (C) Heat map generated using 56 breast cell lines from the CCLE panel showing the levels of expression of IKKα (chuk) and STAT3 downstream targets. (D) Real time PCR showing S1026A induced STAT3 target gene expression. (E) Kaplan-Meier overall survival curves of IKKα in breast cancer patient data set.

**Reference**


1. Lo, H. W., Xia, W., Wei, Y., Ali-Seyed, M., Huang, S. F., and Hung, M. C. (2005) *Cancer research* **65**, 338-348
2. Navolanic, P. M., Steelman, L. S., and McCubrey, J. A. (2003) *International journal of oncology* **22**, 237-252
3. Mendelsohn, J., and Baselga, J. (2003) *J Clin Oncol* **21**, 2787-2799
4. Schlessinger, J. (2002) *Cell* **110**, 669-672
5. Wells, A. (1999) *The international journal of biochemistry & cell biology* **31**, 637-643
6. Cooper, J. A., and Howell, B. (1993) *Cell* **73**, 1051-1054
7. Zwick, E., Hackel, P. O., Prenzel, N., and Ullrich, A. (1999) *Trends Pharmacol Sci* **20**, 408-412
8. Emlet, D. R., Moscatello, D. K., Ludlow, L. B., and Wong, A. J. (1997) *J Biol Chem* **272**, 4079-4086
9. Rojas, M., Yao, S., and Lin, Y. Z. (1996) *J Biol Chem* **271**, 27456-27461
10. Lee, D. F., Kuo, H. P., Chen, C. T., Hsu, J. M., Chou, C. K., Wei, Y., Sun, H. L., Li, L. Y., Ping, B., Huang, W. C., He, X., Hung, J. Y., Lai, C. C., Ding, Q., Su, J. L., Yang, J. Y., Sahin, A. A., Hortobagyi, G. N., Tsai, F. J., Tsai, C. H., and Hung, M. C. (2007) *Cell* **130**, 440-455
11. Feinmesser, R. L., Wicks, S. J., Taverner, C. J., and Chantry, A. (1999) *J Biol Chem* **274**, 16168-16173
12. Winograd-Katz, S. E., and Levitzki, A. (2006) *Oncogene* **25**, 7381-7390
13. Li, X., Huang, Y., Jiang, J., and Frank, S. J. (2008) *Cellular signalling* **20**, 2145-2155
14. Nishimura, M., Shin, M. S., Singhirunnusorn, P., Suzuki, S., Kawanishi, M., Koizumi, K., Saiki, I., and Sakurai, H. (2009) *Molecular and cellular biology* **29**, 5529-5539
15. Heim, M. H. (1999) *Journal of receptor and signal transduction research* **19**, 75-120
16. Lo, H. W., Hsu, S. C., Ali-Seyed, M., Gunduz, M., Xia, W., Wei, Y., Bartholomeusz, G., Shih, J. Y., and Hung, M. C. (2005) *Cancer cell* **7**, 575-589
17. Lo, H. W., Hsu, S. C., Xia, W., Cao, X., Shih, J. Y., Wei, Y., Abbruzzese, J. L., Hortobagyi, G. N., and Hung, M. C. (2007) *Cancer research* **67**, 9066-9076
18. Sakurai, H., Chiba, H., Miyoshi, H., Sugita, T., and Toriumi, W. (1999) *J Biol Chem* **274**, 30353-30356
19. Heisermann, G. J., and Gill, G. N. (1988) *J Biol Chem* **263**, 13152-13158
20. Liu, B., Xia, X., Zhu, F., Park, E., Carbajal, S., Kiguchi, K., DiGiovanni, J., Fischer, S. M., and Hu, Y. (2008) *Cancer cell* **14**, 212-225
21. Kwak, Y. T., Radaideh, S. M., Ding, L., Li, R., Frenkel, E., Story, M. D., Girard, L., Minna, J., and Verma, U. N. (2011) *Molecular cancer research : MCR* **9**, 341-349
22. Marinari, B., Moretti, F., Botti, E., Giustizieri, M. L., Descargues, P., Giunta, A., Stolfi, C., Ballaro, C., Papoutsaki, M., Alema, S., Monteleone, G., Chimenti, S., Karin, M., and Costanzo, A. (2008) *Proceedings of the National Academy of Sciences of the United States of America* **105**, 17091-17096
23. Ettenberg, S. A., Magnifico, A., Cuello, M., Nau, M. M., Rubinstein, Y. R., Yarden, Y., Weissman, A. M., and Lipkowitz, S. (2001) *J Biol Chem* **276**, 27677-27684
24. Bao, J., Gur, G., and Yarden, Y. (2003) *Proceedings of the National Academy of Sciences*

*of the United States of America* **100**, 2438-2443
25. Han, W., Zhang, T., Yu, H., Foulke, J. G., and Tang, C. K. (2006) *Cancer biology & therapy* **5**, 1361-1368
26. Hsu, J. M., Chen, C. T., Chou, C. K., Kuo, H. P., Li, L. Y., Lin, C. Y., Lee, H. J., Wang, Y. N., Liu, M., Liao, H. W., Shi, B., Lai, C. C., Bedford, M. T., Tsai, C. H., and Hung, M. C. (2011) *Nature cell biology* **13**, 174-181
27. Greulich, H., Chen, T. H., Feng, W., Janne, P. A., Alvarez, J. V., Zappaterra, M., Bulmer, S. E., Frank, D. A., Hahn, W. C., Sellers, W. R., and Meyerson, M. (2005) *PLoS medicine* **2**, e313
28. Barretina, J., Caponigro, G., Stransky, N., Venkatesan, K., Margolin, A. A., Kim, S., Wilson, C. J., Lehar, J., Kryukov, G. V., Sonkin, D., Reddy, A., Liu, M., Murray, L., Berger, M. F., Monahan, J. E., Morais, P., Meltzer, J., Korejwa, A., Jane-Valbuena, J., Mapa, F. A., Thibault, J., Bric-Furlong, E., Raman, P., Shipway, A., Engels, I. H., Cheng, J., Yu, G. K., Yu, J., Aspesi, P., Jr., de Silva, M., Jagtap, K., Jones, M. D., Wang, L., Hatton, C., Palescandolo, E., Gupta, S., Mahan, S., Sougnez, C., Onofrio, R. C., Liefeld, T., MacConaill, L., Winckler, W., Reich, M., Li, N., Mesirov, J. P., Gabriel, S. B., Getz, G., Ardlie, K., Chan, V., Myer, V. E., Weber, B. L., Porter, J., Warmuth, M., Finan, P., Harris, J. L., Meyerson, M., Golub, T. R., Morrissey, M. P., Sellers, W. R., Schlegel, R., and Garraway, L. A. (2012) *Nature* **483**, 603-607
29. Dauer, D. J., Ferraro, B., Song, L., Yu, B., Mora, L., Buettner, R., Enkemann, S., Jove, R., and Haura, E. B. (2005) *Oncogene* **24**, 3397-3408
30. van de Vijver, M. J., He, Y. D., van't Veer, L. J., Dai, H., Hart, A. A., Voskuil, D. W., Schreiber, G. J., Peterse, J. L., Roberts, C., Marton, M. J., Parrish, M., Atsma, D., Witteveen, A., Glas, A., Delahaye, L., van der Velde, T., Bartelink, H., Rodenhuis, S., Rutgers, E. T., Friend, S. H., and Bernards, R. (2002) *The New England journal of medicine* **347**, 1999-2009
31. Paez, J. G., Janne, P. A., Lee, J. C., Tracy, S., Greulich, H., Gabriel, S., Herman, P., Kaye, F. J., Lindeman, N., Boggon, T. J., Naoki, K., Sasaki, H., Fujii, Y., Eck, M. J., Sellers, W. R., Johnson, B. E., and Meyerson, M. (2004) *Science (New York, N.Y* **304**, 1497-1500
32. Lynch, T. J., Bell, D. W., Sordella, R., Gurubhagavatula, S., Okimoto, R. A., Brannigan, B. W., Harris, P. L., Haserlat, S. M., Supko, J. G., Haluska, F. G., Louis, D. N., Christiani, D. C., Settleman, J., and Haber, D. A. (2004) *The New England journal of medicine* **350**, 2129-2139
33. Kobayashi, S., Boggon, T. J., Dayaram, T., Janne, P. A., Kocher, O., Meyerson, M., Johnson, B. E., Eck, M. J., Tenen, D. G., and Halmos, B. (2005) *The New England journal of medicine* **352**, 786-792
34. Huang, F., Kirkpatrick, D., Jiang, X., Gygi, S., and Sorkin, A. (2006) *Molecular cell* **21**, 737-748
35. Oved, S., Mosesson, Y., Zwang, Y., Santonico, E., Shtiegman, K., Marmor, M. D., Kochupurakkal, B. S., Katz, M., Lavi, S., Cesareni, G., and Yarden, Y. (2006) *J Biol Chem* **281**, 21640-21651
36. Song, H., Li, C. W., Labaff, A. M., Lim, S. O., Li, L. Y., Kan, S. F., Chen, Y., Zhang, K., Lang, J., Xie, X., Wang, Y., Huo, L. F., Hsu, S. C., Chen, X., Zhao, Y., and Hung, M. C. (2011) *Biochemical and biophysical research communications* **404**, 68-73
37. Goh, L. K., Huang, F., Kim, W., Gygi, S., and Sorkin, A. (2010) *The Journal of cell biology* **189**, 871-883

38. Sordella, R., Bell, D. W., Haber, D. A., and Settleman, J. (2004) *Science (New York, N.Y* **305**, 1163-1167
39. Jiang, L. Q., Feng, X., Zhou, W., Knyazev, P. G., Ullrich, A., and Chen, Z. (2006) *Oncogene* **25**, 5495-5506
40. Karin, M., and Greten, F. R. (2005) *Nature reviews* **5**, 749-759
41. Huang, W. C., Ju, T. K., Hung, M. C., and Chen, C. C. (2007) *Molecular cell* **26**, 75-87
42. Li, C. W., Xia, W., Huo, L., Lim, S. O., Wu, Y., Hsu, J. L., Chao, C. H., Yamaguchi, H., Yang, N. K., Ding, Q., Wang, Y., Lai, Y. J., LaBaff, A. M., Wu, T. J., Lin, B. R., Yang, M. H., Hortobagyi, G. N., and Hung, M. C. (2012) *Cancer research* **72**, 1290-1300

# Figure 1

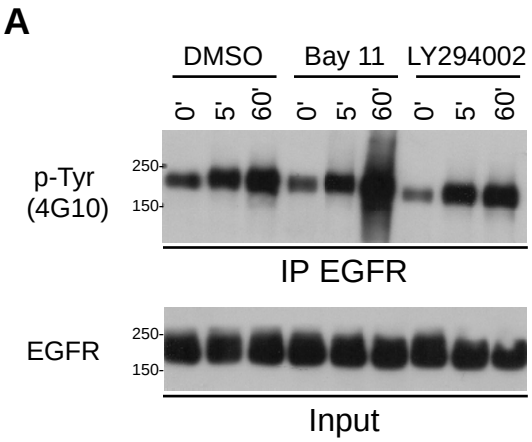


**B**

| Inhibitors | EGFR p-Tyr |
|---|---|
| Bay 11-7082 | ++ |
| Pathenilide | N |
| U0126 | N |
| LY294002 | N |
| PD98059 | N |
| Rapamycin | N |
| AG1478 | ––– |

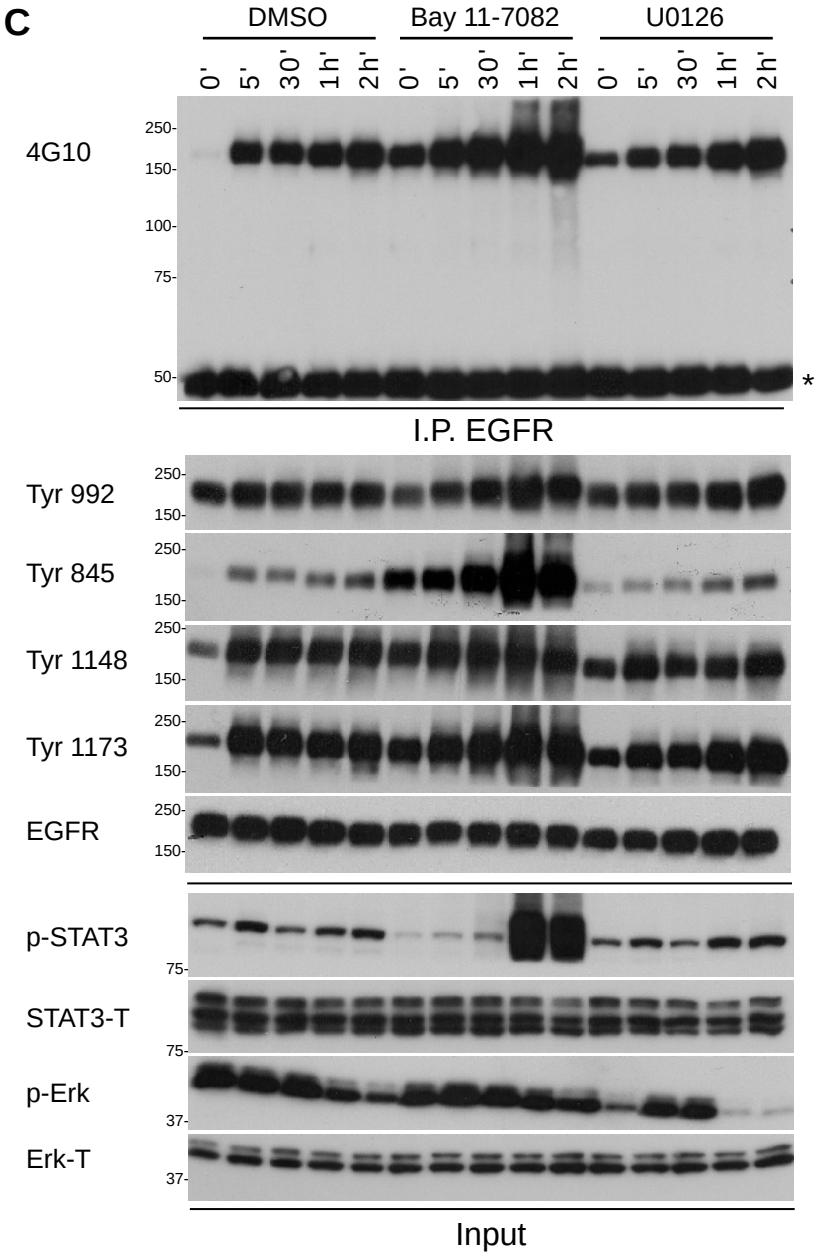


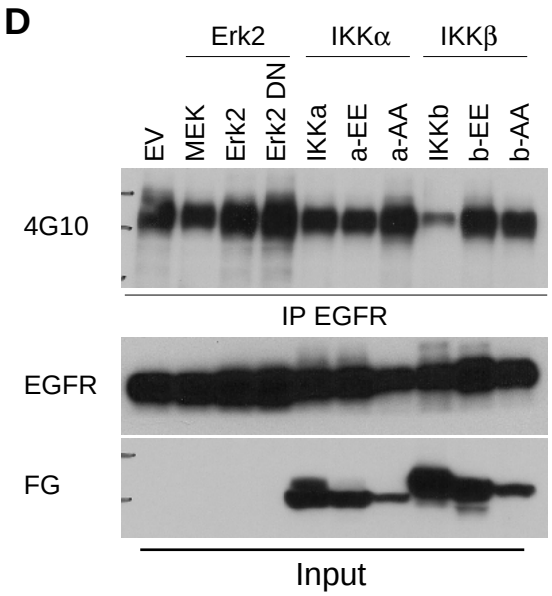


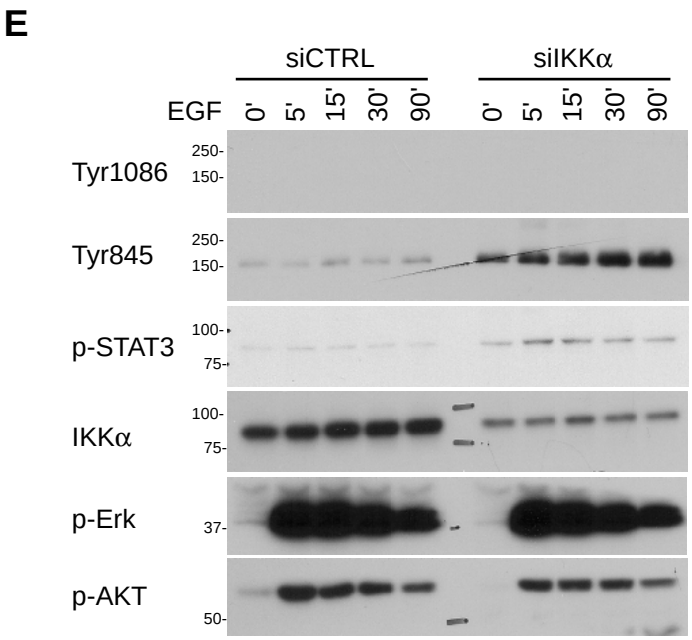

# Figure 2

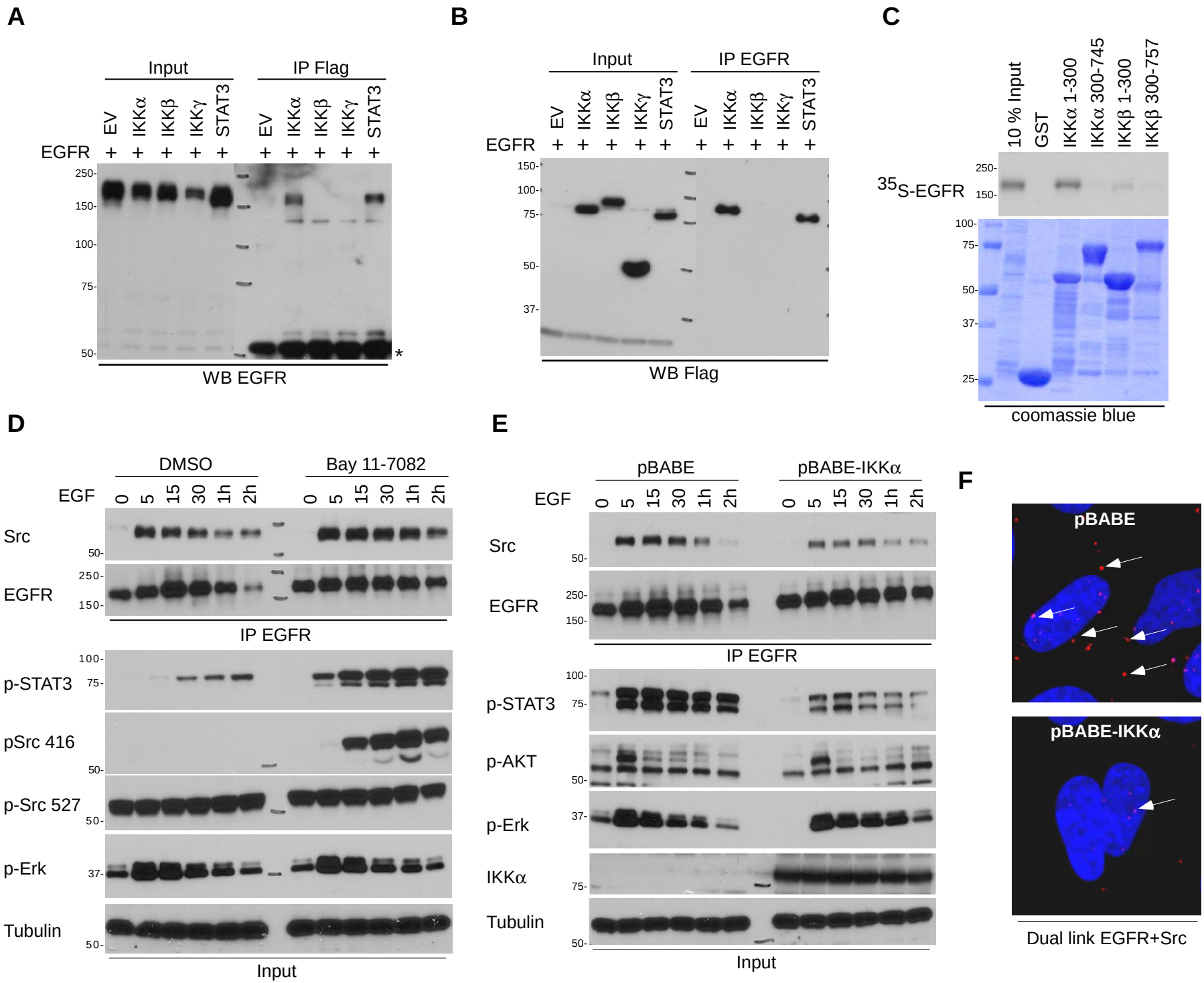
A
Input
IP Flag
EV
IKKα
IKKβ
IKKγ
STAT3
EGFR
250-
150-
100-
75-
50-
*
WB EGFR
B
Input
IP EGFR
WB Flag
37-
C
10 % Input
GST
IKKα 1-300
IKKα 300-745
IKKβ 1-300
IKKβ 300-757
35S-EGFR
25-
coomassie blue
D
DMSO
Bay 11-7082
EGF
0
5
15
30
1h
2h
Src
IP EGFR
p-STAT3
pSrc 416
p-Src 527
p-Erk
Tubulin
Input
E
pBABE
pBABE-IKKα
p-AKT
IKKα
F
pBABE
pBABE-IKKα
Dual link EGFR+Src

# Figure 3

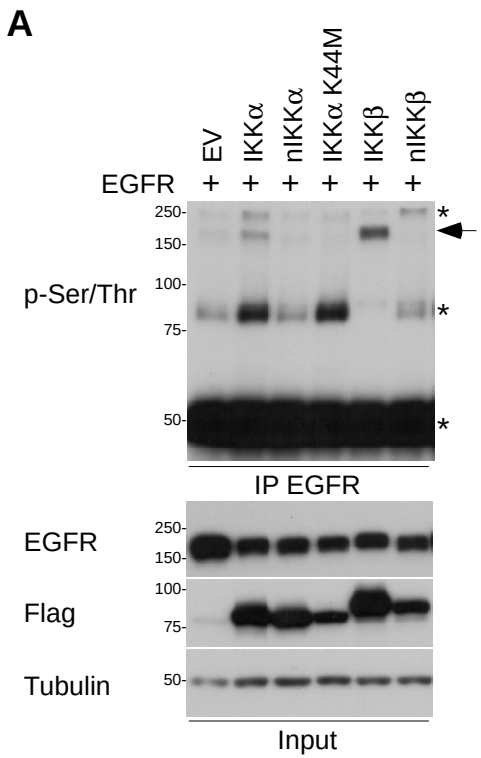
A
EGFR
+ EV
+ IKKα
+ nIKKα
+ IKKα K44M
+ IKKβ
+ nIKKβ
p-Ser/Thr
IP EGFR
EGFR
Flag
Tubulin
Input

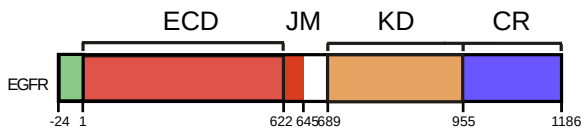
B
ECD
JM
KD
CR
EGFR
-24 1
622 645 689
955
1186

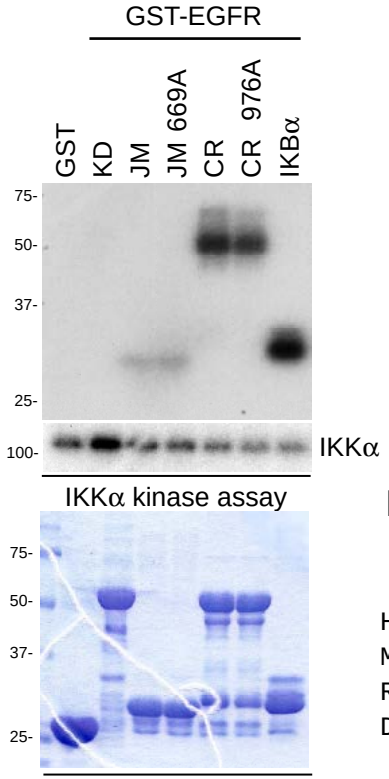
GST-EGFR
GST
KD
JM
JM 669A
CR
CR 976A
IKBα
IKKα
IKKα kinase assay
Coomassie blue

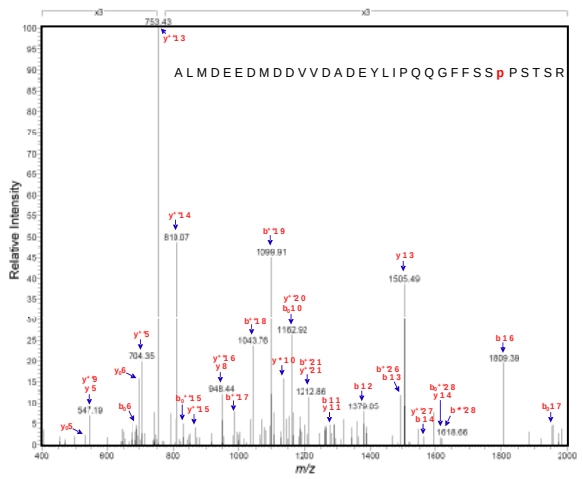
C
ALMDEEDMDDVVDADEYLIPQQGFFSSpPSTSR
Relative Intensity
m/z

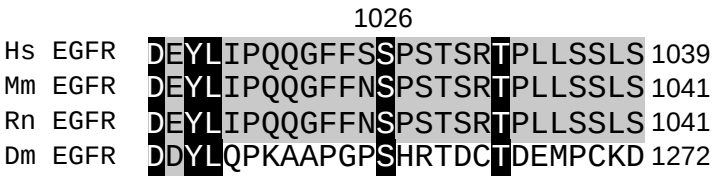
D
1026
Hs EGFR DEYLIPQQGFFSSPSTSRTPLLSSLS 1039
Mm EGFR DEYLIPQQGFFNSPSTSRTPLLSSLS 1041
Rn EGFR DEYLIPQQGFFNSPSTSRTPLLSSLS 1041
Dm EGFR DDYLQPKAAPGPSHRTDCTDEMPCKD 1272

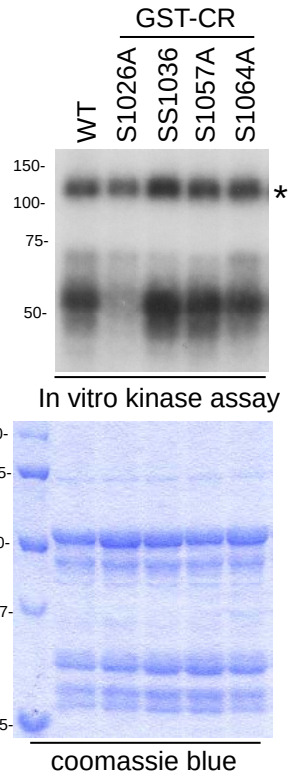
GST-CR
WT
S1026A
SS1036
S1057A
S1064A
In vitro kinase assay
coomassie blue

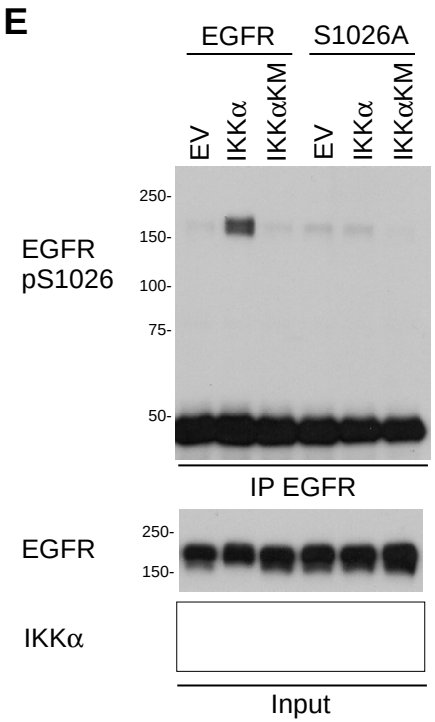
E
EGFR
S1026A
EV
IKKα
IKKαKM
EGFR pS1026
IP EGFR
EGFR
IKKα
Input

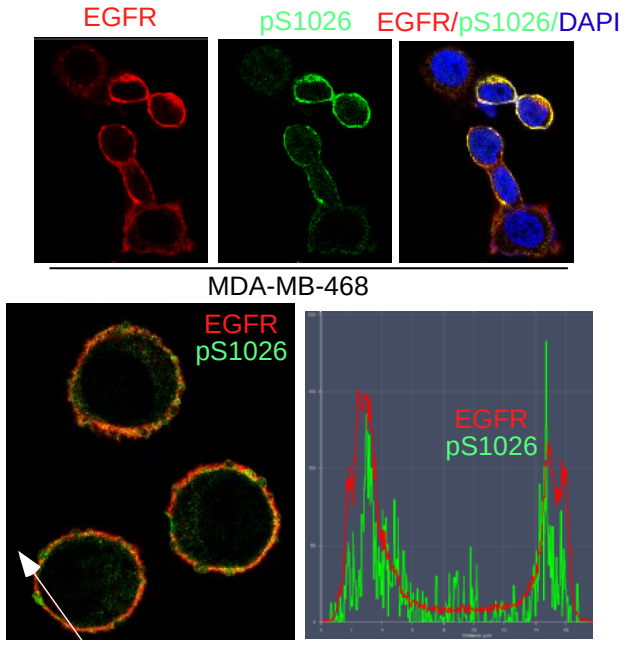
F
EGFR
pS1026
EGFR/pS1026/DAPI
MDA-MB-468
EGFR
pS1026

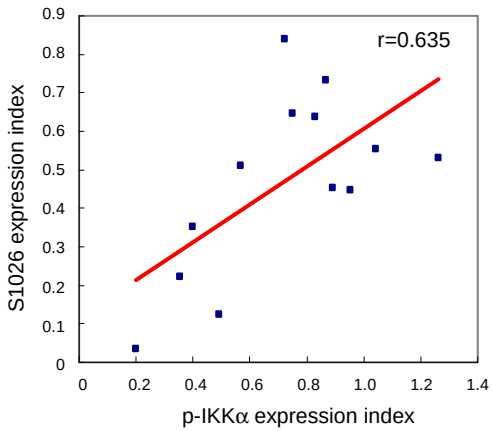
G
r=0.635
S1026 expression index
p-IKKα expression index

# Figure 4

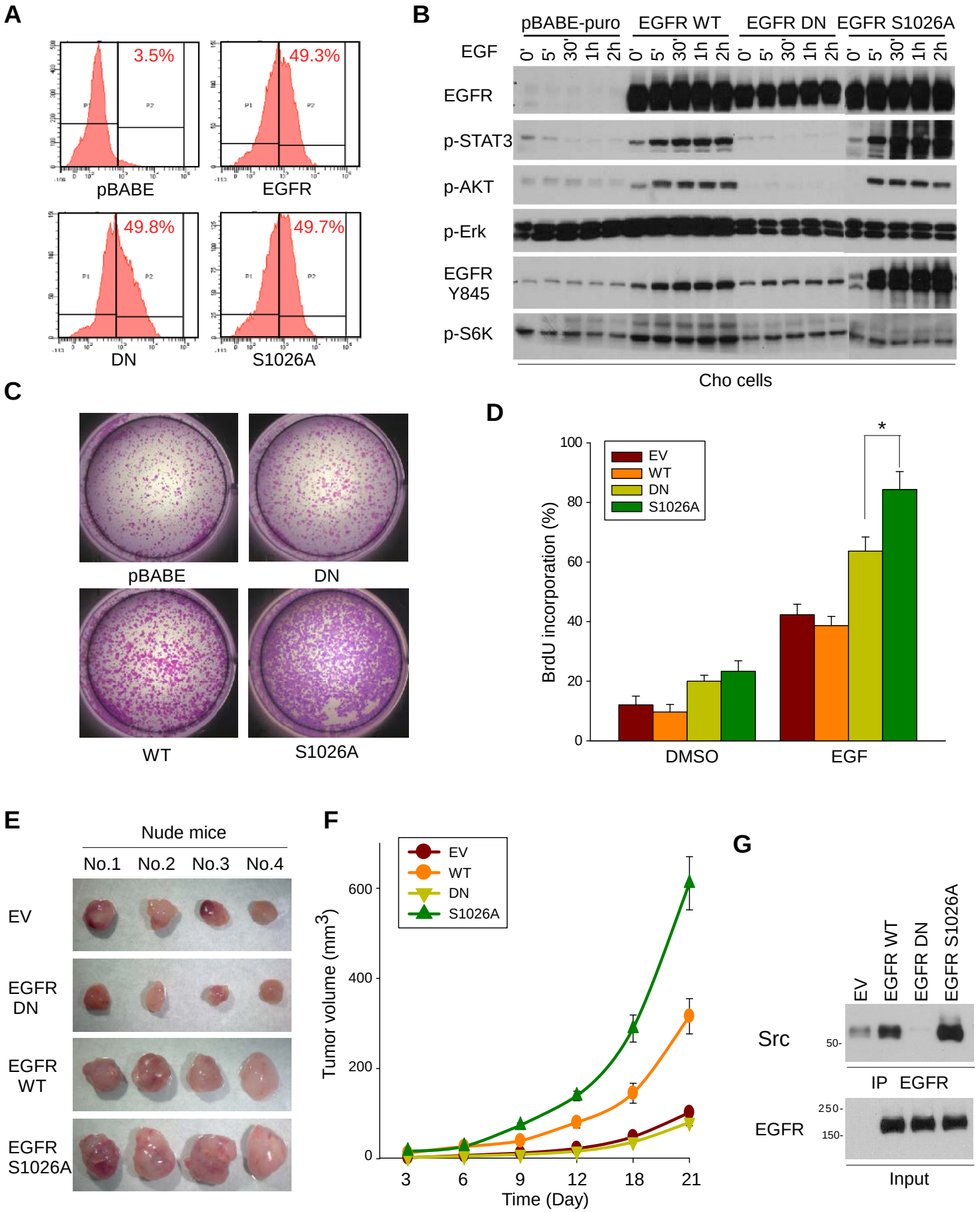
A
3.5%
49.3%
pBABE
EGFR
49.8%
49.7%
DN
S1026A
B
pBABE-puro
EGFR WT
EGFR DN
EGFR S1026A
EGF
0' 5' 30' 1h 2h 0' 5' 30' 1h 2h 0' 5' 30' 1h 2h 0' 5' 30' 1h 2h
EGFR
p-STAT3
p-AKT
p-Erk
EGFR Y845
p-S6K
Cho cells
C
pBABE
DN
WT
S1026A
D
BrdU incorporation (%)
EV
WT
DN
S1026A
*
DMSO
EGF
E
Nude mice
No.1 No.2 No.3 No.4
EV
EGFR DN
EGFR WT
EGFR S1026A
F
Tumor volume (mm3)
EV
WT
DN
S1026A
Time (Day)
G
EV
EGFR WT
EGFR DN
EGFR S1026A
Src
IP EGFR
EGFR
Input

# Figure 5

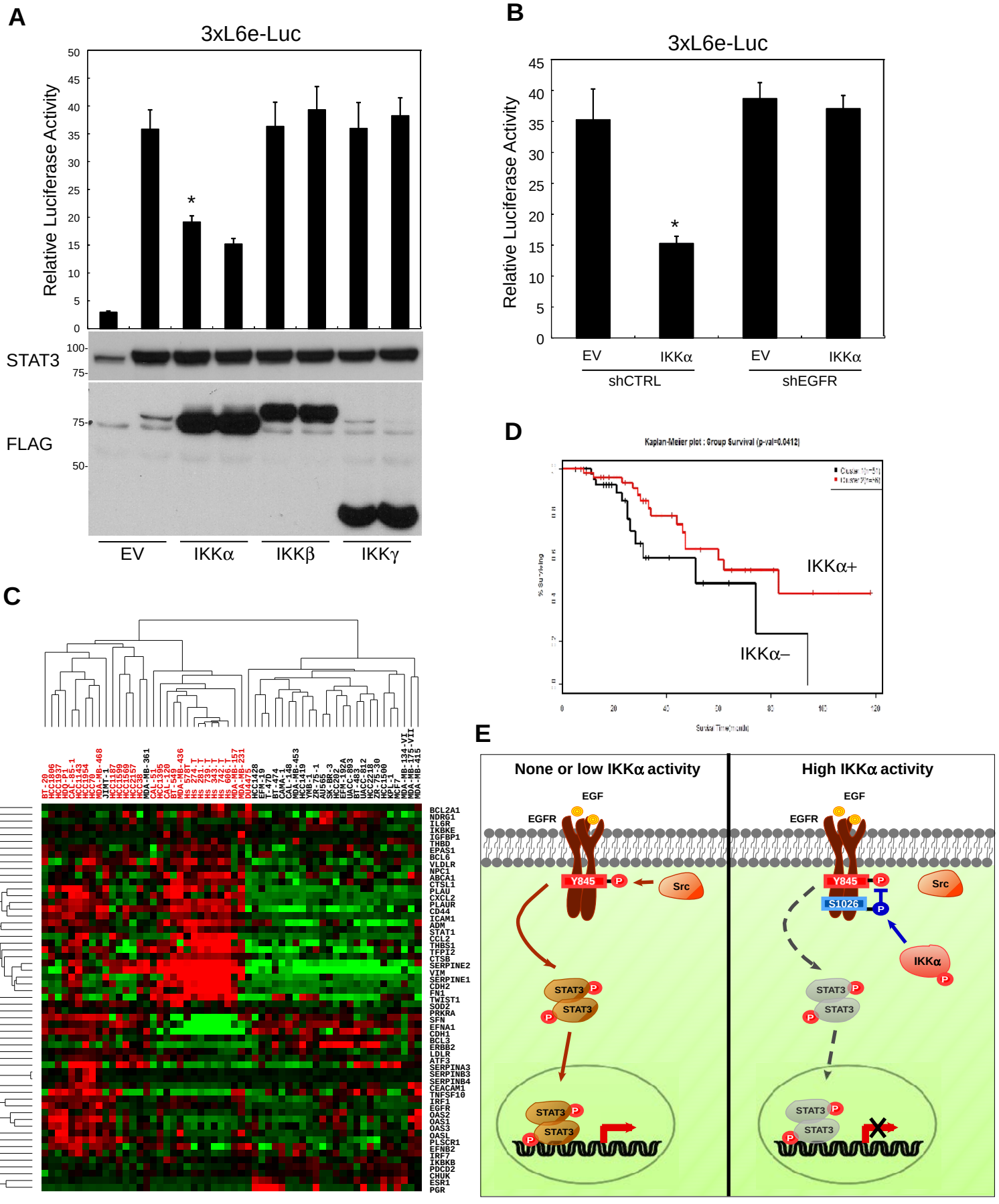
A
3xL6e-Luc
Relative Luciferase Activity
STAT3
FLAG
EV
IKKα
IKKβ
IKKγ
B
3xL6e-Luc
Relative Luciferase Activity
EV
IKKα
EV
IKKα
shCTRL
shEGFR
C
D
Kaplan-Meier plot : Group Survival (p-val=0.0412)
IKKα+
IKKα–
E
None or low IKKα activity
High IKKα activity
EGF
EGFR
Y845
Src
S1026
IKKα
STAT3

# AKT1-mediated Inhibition of Breast Cancer Epithelial-Mesenchyme Transition Requires Phosphorylation-dependent Twist1 Degradation

Running Title: AKT1 induces β-TrCP-mediated Twist1 degradation

Chia-Wei Li[1], Weiya Xia[1], Seung-Oe Lim[1], Jennifer L. Hsu[1,7,8], Longfei Huo[1], Yun Wu[3] , Long-Yuan Li[7], Chien-Chen Lai[6], Shih-Shin Chang[1], Yi-Hsin Hsu[1], Hui-Lung Sun[1], Jongchan Kim[1], Hirohito Yamaguchi[1], Dung-Fang Lee[1], Hongmei Wang[1], Yan Wang[1], Chao-Kai Chou[1,7,8], Jung-Mao Hsu[1], Yun-Ju Lai[2], Adam M. LaBaff[1,5], Qingqing Ding[1], How-Wen Ko[1,5], Fuu-Jen Tsai[6], Chang-Hai Tsai[6], Gabriel N. Hortobagyi[4], and Mien-Chie Hung[1,5,7,8,*]

[1]Department of Molecular and Cellular Oncology, [2]Department of Experimental Therapeutics, [3]Department of Pathology, and [4]Department of Breast Medical Oncology, The University of Texas MD Anderson Cancer Center, Houston, TX 77030, USA

[5]Graduate School of Biomedical Sciences, The University of Texas Health Science Center, Houston, TX 77030, USA

[6]China Medical University, Taichung 404, Taiwan

[7]Center for Molecular Medicine and Graduate Institute of Cancer Biology, China Medical University, Taichung 404, Taiwan

[8]Department of Biotechnology, Asia University, Taichung 413, Taiwan

*Correspondence: Mien-Chie Hung, Department of Molecular and Cellular Oncology, Unit 108, The University of Texas MD Anderson Cancer Center, 1515 Holcombe Blvd., Houston, TX

77030. E-mail: mhung@mdanderson.org

**SUMMARY**

Epithelial-to-mesenchyme transition (EMT) is an essential physiological process that promotes cancer cell migration, invasion, and metastasis. Several lines of evidence from both cellular and genetic studies suggest that AKT1/PKBα, but not AKT2 or AKT3, serves as a negative regulator of EMT and breast cancer metastasis. However, the underlying mechanism by which AKT1 suppresses EMT remains poorly defined. Here, we demonstrate that Twist1 phosphorylated by AKT1 is required for β-TrCP-mediated Twist1 ubiquitination and degradation. The clinically used AKT inhibitor MK-2206, which possesses higher specificity toward AKT1, stabilizes Twist1 and enhances EMT in breast cancer cells. This adverse effect can be overcome by combination therapy of MK-2206 and resveratrol to induce β-TrCP-mediated Twist1 degradation.

## SIGNIFICANCE

The allosteric AKT inhibitor MK-2206 has been studied in multiple clinical trials either as a single agent or in combination with other chemotherapeutics for cancer treatment including breast cancer. Here, we show that AKT1 negatively regulates EMT phenotype by phosphorylating Twist1, a key EMT regulator. However, β-TrCP-mediated degradation of Twist1 combined with MK-2206 treatment also enhances EMT, raising a concern that AKT inhibitor may accelerate metastasis as an anti-cancer agent. We also discovered that resveratrol, a naturally occurring compound, induces β-TrCP to attenuate MK-2206-mediated EMT in breast cancer cells. Given that resveratrol counteracts the unexpected increase in the metastatic potential by anti-AKT therapy, our studies suggest that the addition of resveratrol to anti-AKT therapy may provide extra benefit.

## INTRODUCTION

The AKT/PKB protein kinase family, consisting of AKT1/PKBα, AKT2/PKBβ, and AKT3/PKBγ that are highly conserved cellular homologues with 80% sequence identity, plays critical roles in regulating cell growth, proliferation, and survival, among many other cellular events (Datta et al., 1999). Amplification, overexpression, and somatic mutations of AKT and its upstream regulator phosphatidylinositol-3 kinase (PI3K) as well as deletion or inactive mutations of PTEN have been found in various human cancer types. Because activation of AKT signaling is believed to promote tumorigenesis (Manning and Cantley, 2007), multiple drugs targeting the PI3K/AKT pathway have been tested as anti-cancer drugs in clinical trials (Lindsley, 2010).

Structurally, all members of the AKT family share a common domain organization that consists of a variable N-terminal pleckstrin homology domain and a short alpha-helical linker region, followed by a central kinase domain and a C-terminal hydrophobic regulatory region (Yang et al., 2002) (Huang et al., 2003). The kinase domain is responsible for the oncogenic activity of AKT via direct interaction with and phosphorylation of its downstream targets. It is known that AKT phosphorylates substrates at a serine or threonine residue in a conserved RxRxxS/T motif characterized by arginine at positions -5 and -3 (Alessi et al., 1996). Through protein phosphorylation, AKT has been shown to either positively or negatively regulate substrate activity, alter subcellular localization, or affect protein stability (Manning and Cantley, 2007). While a number of AKT substrates, including GSK-3β (Cross et al., 1995), MDM2 (Zhou et al., 2001), p21 (Zhou et al., 2001), and EZH2 (Cha et al., 2005) have been well characterized, others remain to be discovered.

AKT family members have long been thought to promote tumor initiation and cell progression and are considered excellent targets for anti-cancer therapy. However, emerging

evidence suggests a negative role of AKT1 in navigating tumor metastasis in breast cancer cells (Dillon and Muller, 2010). For instance, siRNA knockdown of AKT1 but not AKT2 in insulin-like growth factor-1 (IGF-1)-stimulated cells promotes epithelial-to-mesenchyme transition (EMT) and cell migration (Irie et al., 2005). In addition, overexpression of AKT1 in breast cancer cells blocks cell motility and invasion (Irie et al., 2005) (Yoeli-Lerner et al., 2005). Most recently, downregulation of AKT1 in MCF 10A cells was shown to decrease miR-200 abundance, thereby promoting transforming growth factor-β-induced EMT and stem cell-like phenotype (Iliopoulos et al., 2009). Additionally, in $AKT1^{-/-}$ and ErbB2 transgenic mice, AKT1 inhibited tumor invasion and metastasis but accelerated mammary tumorigenesis (Hutchinson et al., 2004).

The nonredundant mechanism by which AKT1 but not AKT2 inhibits metastasis remains largely unknown even though many of the physiological consequences have been unraveled. Thus far, AKT1 has been shown to activate the MDM2-mediated ubiquitination and degradation of nuclear factor of activated T-cells (NFAT1), which inhibits breast cancer cells migration and invasion (Yoeli-Lerner et al., 2005). Phosphorylation and degradation of targeting tumor suppressor tuberous sclerosis complex 2 (TSC2) by AKT1 reduces breast cancer cell motility and invasion (Liu et al., 2006). Moreover, AKT1 but not AKT2 specifically phosphorylates palladin, an actin-bundling protein, to block breast cancer cell migration (Chin and Toker, 2010). These results provide some mechanistic insight into how AKT1 negatively regulates the metastatic activity of breast cancer cells.

EMT, a complex reprogramming process of epithelial cells, plays an indispensable role in tumor invasion and metastasis (Thiery, 2002). The well-defined features of EMT include the loss of epithelial markers (E-cadherin and α- and γ-catenin), the gain of mesenchymal cell markers

(fibronectin, vimentin, and N-cadherin), and the acquisition of migratory and invasive properties (Thiery, 2002) (Huber et al., 2005). To date, several transcriptional repressors, such as Zeb-1/2, Twist1, and Snail-1/2, are known to be involved in EMT regulation. Once activated, these transcription factors recruit histone deacetylases to the E-box elements of the E-cadherin promoter and suppress E-cadherin expression, resulting in the loss of cell adhesion ability (Peinado et al., 2007). Twist1, a highly conserved basic helix-loop-helix (bHLH) transcriptional repressor, induces EMT to facilitate breast tumor metastasis (Yang et al., 2004). Despite frequent reports of Twist1 transcriptional regulation involving EGFR/STAT3 (Lo et al., 2007) (Cheng et al., 2008) and NFκB signaling (Li et al., 2012), the posttranslational regulation of Twist1 remains less understood.

To improve our understanding of AKT1-mediated EMT repression, we cross-analyzed gene expression profile of AKT isoforms using several public datasets. We observed that low expression of AKT1 was highly associated with aggressive breast cancers and poor disease outcome. Unlike AKT2, AKT1 specifically interacted with and phosphorylated Twist1 at three serine/threonine sites, and mutation of these AKT1 phosphorylation sites of Twist1 so they can no longer be phosphorylated, induced strong EMT potential. Moreover, AKT1 also induced a phosphorylation-dependent ubiquitination and degradation of Twist1, engaging the proteasome to Twist1-mediated EMT regulation. Importantly, chronic exposure to anti-AKT inhibitor (MK-2206) induced Twist1 stabilization and EMT in breast cancer cells. Administration of resveratrol, a β-TrCP inducer reduced shAKT1-mediated metastatic potential. Our findings not only establish a molecular interpretation of the role of AKT1 in EMT inhibition but also identify the potential adverse effect utilizing anti-AKT inhibitor for breast cancer treatment.

## RESULTS

### Pathological expression of AKT isoforms in breast cancer cells

Activation of AKT has been shown to correlate with unfavorable clinical prognosis in many cancers including breast cancer. However, due to the lack of isoform specific phospho-AKT antibody, the roles of AKT isoforms in the pathogenesis of breast cancer or their therapeutic potential have not been established. To address these issues, we examined gene expression profile of AKT isoforms using public dataset generated from 917 cancer cell lines (CCLE) (Barretina et al., 2012). We first categorized them into epithelial and mesenchymal subtype based on the gene expression profile of CDH1, CDH2, vimentin, and fibronectin. While AKT2 mRNA levels remain unchanged, AKT1 showed significant downregulation in breast cancer and stomach cancer cells in the mesenchymal subtype (Figure S1A). AKT3 was upregulated in multiple cancers (Figure S1B). To further dissect the expression of AKT isoforms in breast cancer cell lines, unsupervised hierarchical clustering analysis was performed based on the ErbB2, ERα (ESR1), PR (PgR), and EMT profiles. Strikingly, we were able to distinguish basal-like from luminal type breast cancer cells with high accuracy (90% properly segregated) from the gene list (Figure 1A) based on their genetic characteristics. We further found that AKT1 was expressed at a lower level in either aggressive basal-like (vs. luminal) or mesenchymal-type breast cancer cells (vs. epithelial-type) (Figure 1B, middle and right) whereas AKT3 was expressed at a significantly higher level. A similar observation was made when we analyzed another breast cancer dataset containing 54 cell lines (Neve et al., 2006): basal-like or mesenchymal breast cancer cells showed positive correlation with higher expressions of AKT3 whereas the expression of AKT1 showed an inverse correlation (Figures S1C and S1D). Next, we asked whether the clinical distinct group of patient samples also share the differential

expression pattern of AKT isoforms and found similar correlation using the Netherlands Cancer Institute (NKI) dataset (van de Vijver et al., 2002) (Figure 1C) and the University of North Carolina (UNC) cohort (Hu et al., 2006; Oh et al., 2006; Parker et al., 2009) (Figure 1D). While co-expression of AKT1, AKT2 and AKT3 showed no correlation with any breast cancer subtypes (Figure 1C and 1D, left panel), the negative correlation between AKT1 and aggressive phenotype remains significant (Figures 1C and 1D, middle and right). To consolidate the differential regulation between the AKT isoforms, we transiently expressed each myr-AKT isoform and found that myr-AKT1 had similar kinase activity with myr-AKT2 (Figure S1E) but only myr-AKT1 activated E-cadherin reporter robustly (Figure 1E). Consistently, overexpression myr-AKT1 but not myr-AKT2 or myr-AKT3 in MDA-MB-231 cells recapitulated the association of AKT isoforms and EMT regulation (Figure 1F). To further investigate our findings at the protein level, we examined the expression of AKT isoforms in the metastatic breast cancer cohort (MD Anderson Cancer Center) using immunohistochemical (IHC) staining. While the recurrence-free survival (RFS) of patients with higher expression of p-AKT S473, which represents the phosphorylation level of all three AKT1, 2 and 3 isoforms, was significantly worse than patients with lower expression, and this was consistent with most literatures (Figure 1G). Interestingly, the expression of total AKT1 correlated with better patient survival (Figure 1H). The results from these analyses indicate that each of the three AKT isoforms has a distinct pathological profile that is highly relevant to its functionality.

**Twist1 physically associates with AKT1**

Given the distinct regulatory nature of AKT isoform in breast cancer cells, we sought to distinguish their functionality through identifying their specific interacting partners. To test this,

HA-myr-AKT1 and HA-myr-AKT2 were stably expressed in MDA-MB-231 cells. The associated protein complexes were then immunoprecipitated and separated on the SDS-PAGE. As shown in Figure S2A, AKT1 but not AKT2 pulled down a significant amount of a protein appearing at 20 kDa. Mass spectrometry analysis further identified Twist1 as AKT1-specific interacting partner (with 72% sequence coverage). To confirm their interaction at the endogenous level, co-immunoprecipitation analysis (Co-IP) was conducted using MDA-MB-435 cells in which Twist1 is highly expressed. As expected, endogenous AKT1 interacted with endogenous Twist1 (Figures S2B and S2C). To examine whether they interact by a direct physical contact, an *in vitro* GST pull-down assay was performed. Consistently, we found that Twist1 interacted directly with GST-AKT1 but not with GST-AKT2 or GST alone *in vitro* (Figure S2D). Together, these results identify a strong physical interaction between AKT1 and Twist1. Although AKT2 did not show strong interaction with Twist1, these results does not exclude the "hit and run" mechanism for AKT2-mediated Twist1 phosphorylation.

Because the inhibitory nature of AKT1 in the EMT, we asked whether AKT1 represses EMT via the regulation of EMT mediators, such as Twist1, FOXC2, E12, and Snail. To do this, we transiently transfected HEK-293T cells with HA-myr-AKT1 together with Flag-Twist1, Flag-Snail, Flag-FOXC2, or Flag-E12 and investigated the interactions between AKT1 and these EMT mediators. Co-IP analysis revealed that AKT1 associated with Twist1 but not with the other EMT mediators (Figure S2E). Similar results were also obtained in a reverse IP experiment, which showed that AKT1 but not GSK3β, IKKα, or IKKβ, interacted with Twist1 (Figure S3A). Altogether, these results indicate AKT1 interacts with Twist1 and raise an interesting possibility that AKT1-mediated EMT repression maybe regulated through the physical and functional interaction with Twist1.

**AKT1 phosphorylates Twist1 *in vitro***

Since AKT1 interacts directly with Twist1, we next examined whether Twist1 is a physical substrate of AKT1. Twist1 contains two potential AKT phosphorylation motifs (S42 and T121/S123), and these motifs are highly conserved across species (Figure 2A and S3B); therefore, we asked which of these two motifs might be phosphorylated by AKT1. To do so, GST-Twist1 was expressed in two separate fragments: one containing amino acids 1-112 and the other 113-202 (Figure 2B). We then tested them for phosphorylation by AKT1 using an *in vitro* kinase assay. Both GST-Twist1 fragments were strongly phosphorylated by AKT1 (Figure 2C); however, site-directed mutation of each consensus motif on the Twist1 fragments completely abolished their phosphorylation. To pinpoint the phosphorylation potential in context of full-length Twist1, GST-Twist1 S42A (S42A), VA (T121V/S123A) and AVA (S42A/T121V/S123A) mutants were generated and tested for phosphorylation using an *in vitro* kinase assay. We found that substitutions in both AKT phosphorylation motifs (Twist1 AVA) eliminated AKT1-mediated phosphorylation entirely (Figure 2D). In contrast, substitutions in one or the other motif (S42A or T121V/S123A) had little or no effect on the phosphorylation level (Figure 2D). Thus, these results suggest that the three amino acid residues spanning these two AKT phosphorylation motifs in Twist1 (S42, and T121/S123) are required for complete phosphorylation by AKT1 *in vitro*.

**AKT1 phosphorylates Twist1 *in vivo***

To recapitulate AKT1-mediated Twist1 phosphorylation *in vivo*, Flag-Twist1 together with HA-tagged wild-type AKT1 (WT), dominant negative AKT1 (DN), or myr-AKT1 (a

constitutively active form of AKT1) were coexpressed in HEK-293T cells. The cell lysates were then subjected to IP with anti-Flag antibody. Phosphorylation of Twist1 was detected using phospho-AKT substrate antibody and phospho-RxRxxS/T antibody. Twist1 was highly phosphorylated in the presence of myr-AKT1 but not in the presence of AKT1 DN (Figures S3C). Similar to the observations *in vitro* (Figure 2D), mutation of either S42 alone or both T121/S123 in Twist1 did not affect its overall level of phosphorylation by AKT1, whereas mutation of all three sites completely abrogated phosphorylation (Figure 2E). Since protein phosphorylation sometimes results in a mobility shift in SDS-PAGE, we used a phospho-tag to capture phospho-residue during protein migration. We found that myr-AKT1 induced a noticeable mobility shift in Twist1 but not Snail in the absence of λ-phosphatase. In contrast, mutation of all three sites (Twist1-AVA) completely abolished AKT1-induced slow migration of Twist1 (Figure 2F). Consistent to the AKT1 interacting with Twist1 among the EMT regulators (Figure S2E), AKT1 specifically catalyzed Twist1 phosphorylation (Figure S3D). In addition, we found AKT1 and AKT2 governed Twist1 functionality though differential phosphorylation capability such that AKT2 primarily phosphorylates Twist1 at S42 based on *in vitro* kinase assay, which is consistent to a previous study by Vichalkovski et al.(Vichalkovski et al., 2010) (Figure S3E) while AKT1 phosphorylated Twist1 at all three sites (Figure 2F) both *in vitro* and *in vivo* (Figure 2D, 2E and 2F).

To further investigate whether AKT1-mediated Twist1 phosphorylation is PI3K/AKT dependent, we pretreated cells with IGF-1 with or without an AKT inhibitor, MK-2206. Indeed, MK-2206 inhibited IGF-1-induced phosphorylation of Twist1, suggesting that Twist1 phosphorylation is regulated by PI3K signaling cascade (Figure 2G). Although an earlier study showed Twist1 S123 could be phosphorylated by PKA (Vichalkovski et al., 2010), we sought to

determine whether AKT1 also facilitates phosphorylation of this particular residue *in vivo*. To do so, we transiently transfected HeLa cells with HA-Twist1 and myr-AKT1. Phosphorylated Twist1 was then subjected to IP and mass spectrometry. In addition to the previously identified S42 phosphorylation site (data not shown) (Vichalkovski et al., 2010), we successfully identified a novel S123 phosphorylation *in vivo* (Figure S3F). Endogenous Twist1 phosphorylation by total AKT was also detected in various cancer cell lines (Figure S3G) using a phospho-RXRXXS/T substrate antibody. Collectively, our results suggest that all three residues spanning both AKT motifs are responsible for Twist1 phosphorylation, and mutation of all three is required to abolish phosphorylation by AKT1. To understand AKT1/2-mediated Twist1 phosphorylation, we re-expressed AKT1 or AKT2 silence mutant that encodes a WT protein in the AKT1/2/3 knockdown cells. To do so, AKT1, AKT2, and AKT3 were specifically knocked down in MDA-MB-231 cells using pGZIP vector (Figure S3H). AKT1 WT, AKT1 KD, AKT2 WT, and AKT2 KD were then overexpressed using the same shRNA backbone under CMV promoter (Figure S3I). Cells that re-expressed AKT1 had Twist1 S42, T121 and S123 phosphorylation, whereas those re-expressing AKT2 only had Twist1 phosphorylation at S42 (Figure S3J).

**Phosphorylation by AKT1 is required for Twist1 degradation**

Since AKT1 phosphorylates Twist1, we asked how AKT1 affects Twist1 expression. We noticed that the expression level of Twist1 was higher in AKT1-deficient MEFs compared with WT MEFs (Figure 3A), and ectopic expression of AKT1 but not AKT2 downregulated Twist1 expression in the HeLa cells stably expressing myr-AKT1 and AKT2, even though activation of both AKT1 and AKT2 were appropriately regulated by phosphorylation of GSK3β (Figure 3B). Downregulation of AKT1 but not AKT2 by shRNA also upregulated Twist1 expression (Figure

3C, right). Consistent with an earlier study (Iliopoulos et al., 2009), silencing AKT1 but not AKT2 expression induced EMT phenotypic change in MCF 10A cells (Figure 3C, left). Together, these results suggest that AKT1 but not AKT2 activation negatively regulates Twist1 expression (Figure 3C).

Next, we measured the protein turnover rate in the presence of cycloheximide to determine the effect of AKT1-mediated phosphorylation on Twist1 protein stability. The turnover rate of Twist1 in myr-AKT1 expressing cells was much more rapidly compared with those in myr-AKT2 expressing or empty vector control cells (Figure 3D). We further examined the protein half-life of Twist1 and its three phospho-deficient variants (S42A, VA, and AVA) and found that the half-life of Twist1 AVA was significantly longer compared to that of Twist1 WT and Twist1 DDD phosphorylation-mimic mutant in the presence of myr-AKT1 (Figure 3E). These results suggest that AKT1-repressed Twist1 expression is likely mediated through phosphorylation of Twist1 by AKT1.

The reduced half-life of Twist1 by AKT1-mediated phosphorylation prompted us to ask whether it is accompanied by 26S proteasome-mediated degradation. Indeed, treatment of MG132 stabilized Twist1 expression in the multiple cell lines (Figure S4A), supporting the notion. Since one hallmark of protein degradation is the conjugation of polyubiquitin chain(s), we next asked whether AKT1 regulates Twist1 via ubiquitination. HEK-293T cells were transiently transfected with HA-Twist1 WT or mutants together with His-Ub or His-Ub plus myr-AKT1. Ubiquitinated Twist1 was then pulled down by $Ni^{2+}$ agarose beads under intense denaturing conditions and subjected to Western blot analysis. Twist1 was reported to have notable basal ubiquitination (Demontis et al., 2006) (Brunet et al., 1999), coexpression of myr-AKT1 but not myr-AKT2 or myr-AKT3 stimulated ubiquitination of Twist1 (Figure S4B).

Interestingly, AKT1-induced Twist1 ubiquitination was abolished in the AVA mutant, suggesting that AKT1-mediated Twist1 phosphorylation is required for Twist1 ubiquitination. We showed that IGF-1 induced Twist1 downregulation was abrogated by AKT1 but not AKT2 suppression (Figure 3F). In addition, a negative correlation between AKT1 and Twist1 expression was found in 13 human breast cancer cell lines, suggesting that high AKT1 expression promotes Twist1 destabilization (Figures 3G and S4C). These results suggest that AKT1-mediated Twist1 phosphorylation induces Twist1 polyubiquitination and degradation via the 26S proteasome machinery.

**AKT1 modulates β-TrCP-mediated Twist1 degradation**

To further investigate how Twist1 is degraded, it is of interest to identify the ubiquitin E3 ligase that regulates Twist1 stability. To this end, we noted that Twist1 contains one β-TrCP destruction box, DSΨXXS, which is also present in β-catenin, IκB, and Snail (Figure 4A) (Guardavaccaro et al., 2003; Margottin-Goguet et al., 2003). Overexpression of β-TrCP induced a rapid degradation of Twist1 (Figure S5A) and mutation of this motif (DSLSNS to DALSNA) (Figures 4B) or knockdown of β-TrCP (Figures S5B) stabilized Twist1 expression. Similar to many β-TrCP substrates, induction of β-TrCP expression in MDA-MB-468 (Figure 4C) and HeLa cells (Figure S5C) by ciglitazone (CG), troglitazone (TG), or resveratrol (Wei et al., 2009; Wei et al., 2007) reduced Twist1 expression, supporting that β-TrCP upregulation mediates Twist1 degradation. Because β-TrCP mainly regulates cell cycle S phase entry (Busino et al., 2003), we asked whether Twist1 expression is regulated during cell cycle progression. Using a double thymidine (Figure 4D, quantitation of S5D) and thymidine/nocodazole assay (Figure S5E), we found that Twist1 protein but not mRNA was degraded during S to G2/M phase. In

addition, downregulation of β-TrCP expression stabilized Twist1, which suggests that β-TrCP is an authentic E3 ligase regulating Twist1 degradation at S phase.

To further validate whether AKT1 is involved in β-TrCP-mediated Twist1 destabilization, we expressed β-TrCP WT or β-TrCP ΔF (a β-TrCP variant that lacks the F-box domain) in HEK-293T cells to test their ability to induce Twist1 WT and AVA ubiquitination. We found that β-TrCP, but not β-TrCP ΔF, induced specific ubiquitination of Twist1 WT whereas Twist1 AVA could not be ubiquitinated (Figure 4E). In addition, co-expression of β-TrCP facilitated AKT1-mediated Twist1 degradation (Figure 4F). Because there is abundant degradation machinery in the cytoplasm, we asked whether AKT1-mediated Twist1 phosphorylation also occurs in specific subcellular localization. When we examined cellular localization of WT and mutants Twist1, we found that Twist1 WT and Twist1 DDD localized mainly to the nucleus with visible expression in the cytoplasm (Singh and Gramolini, 2009) using fluorescence microscopy (Figures 4G and S4D) and cell fractionation analysis (Figure 4H). Twist1 AVA, which is resistant to 26S proteasome-mediated degradation, localized exclusively in the nucleus. The results suggest that AKT1-mediated phosphorylation of Twist1 is required for its translocation from the nucleus to the cytoplasm for degradation. In this regard, it is worthwhile to mention another EMT transcription factor, Snail, is also regulated by GSK3β in a similar fashion (Zhou et al., 2004).

**Twist1 AVA is a potent inducer of EMT**

Because Twist1 is a key mediator during EMT progression, we also investigated the effect of AKT1-mediated Twist1 phosphorylation in EMT using Twist1 phosphorylation-deficient (Twist1 AVA) and phosphorylation-mimic (Twist1 DDD) mutants. To this end, we established stable transfectants with empty vector (EV), Twist1 WT, and AVA and DDD Twist1 mutants in MCF7

breast cancer cells, in which the basal level of endogenous Twist1 WT is low. Of the 35 clones screened, more than 15 clones expressed Twist1 WT, and E-cadherin was only partially or not downregulated with no apparent morphological changes that resemble EMT. Likewise, the Twist1 DDD stable transfectants did not induce any E-cadherin loss or EMT phenotype. Interestingly, half of the 20 neomycin-resistant clones of Twist1 AVA transfectants underwent morphological changes that resembled EMT. Stable transfectants with similar Twist1 expression levels were used for comparison (Figures 5A, 5B, S6A, and S6B). To exclude the effects of clonal selection in the stable transfectants, we infected MDCK cells with replication-incompetent retroviruses expressing Flag-Twist1 WT, AVA, and DDD. In both MCF7 and MDCK cells, Twist1 AVA induced a significant downregulation of E-cadherin and a gain of N-cadherin expression (Figures 5A, 5B and S6C). Another fibroblast marker, vimentin, was also selectively expressed in the Twist1 AVA cells (Figures 5B, and S6B). Real time-PCR analysis showed that the mRNA level of E-cadherin was partially reduced in MCF7-Twist1 WT cells but completely abrogated in MCF7-Twist1 AVA cells (Figure 5C). These results suggest that AKT1-mediated phosphorylation reduces DNA binding activity of Twist1 that results in derepression of Twist1-repressed E-cadherin.

Since EMT is associated with acquisition of cell motility, we performed a Transwell invasion assay to validate the increase in the motility of the stable clones. Although cell proliferation rate of Twist1 variants remained similar (Figures S6D and S6E), cell invasion ability was significantly enhanced in MCF7 Twist1 AVA transfectants (Figure 6F). We also performed a wound-healing assay to track the movement of MCF7 stable transfectants using time-lapse microscopy. After 24-hr incubation, MCF7-Twist1 AVA cells displayed accelerated migration into the wound compared to the WT and DDD mutant (Figure S7A). We quantitated

the number of migrating cells (Figure S7B). Similarly, Twist1 AVA showed aggressive phenotype. To further validate the migration ability was due to the loss of E-cadherin, we restored E-cadherin into two independent Twist1 AVA clones to revert Twist1 AVA-induced EMT (Figure S7C). Because EMT is usually accompanied by an increase in cancer stem cell properties, we also conducted stem cell analysis and found that Twist1 AVA had a higher ability to induce cancer stem cell side population (Figure 5D) and mammosphere formation (Figure 5D, inset) compared with WT and DDD. Moreover, the motile behavior of Twist1 AVA also reflected its anti-apoptosis ability. Unlike Twist1 S42A and VA, which showed minor effect from adriamycin-induced apoptosis, Twist1 AVA significantly protected cells from apoptosis (Figure S7D). Taken together, abrogation of AKT1-mediated Twist1 phosphorylation enhances EMT phenotypic changes that resemble AKT1-induced EMT repression.

To consolidate the role of Twist1 in AKT1-mediated EMT repression, we knocked down Snail and Twist1 in shAKT1 clone and found that downregulation of Twist1 but not Snail abolished shAKT1-induced EMT (Figure S7E). We also stably expressed myr-AKT1 DN (dominant negative myr-AKT1) in MCF 10A (shCTRL) and two Twist1 knockdown stable clones (shTW-1 and shTW-2) (Li et al., 2012). Myr-AKT1 DN increased Twist1 expression and enhanced TGFβ-induced EMT as measured by downregulation of E-cadherin and upregulation of vimentin and N-cadherin expression. However, knocking down Twist1 inhibited TGFβ-induced EMT in AKT1 DN expressing cells, whereas cells that received shCTRL showed no effect (Figure 5E). Thus, expression of Twist1 expression in MCF 10A cells is required for TGFβ/myr-AKT1 DN-induced EMT. We next validated this finding through a lung colonization xenograft model. The *in vivo* experimental metastasis assay showed that myr-AKT1 DN expression in 4T1-Luc cells enhanced metastatic potential as measured by the number of lung

colonization, and knockdown of Twist1 expression antagonized myr-AKT1 DN-induced metastasis (Figure 5F). To better delineate the role of Twist1 in breast cancer metastasis, we used mouse model that develops spontaneous metastasis to measure the impact of Twist1. MDA-MB-231 cells harboring shAKT1 or shTwist1 were laterally injected to the mammary gland of 6-week-old female mice. Primary tumors were removed after three weeks of tumor cell injection. The rate of metastasis was determined by measuring lung nodules formation. As shown in Figure 5G, downregulation of AKT1 reduced tumor growth but induced aggressive lung metastasis. Indeed, AKT1 mediated EMT inhibition required Twist1, because downregulation of Twist1 impaired shAKT1-mediated metastasis (Figure 5H and 5I).

**AKT1 controls the molecular switch by T121 and S123 phosphorylation**

To differentiate AKT2-induced EMT via Twist1 S42 phosphorylation, a series of functional analyses was performed to distinguish the isoform-specific regulation in the context of Twist1. As shown in Figure 6, Twist1 S42A (AKT2-deficient mutant) showed similar stability (Figure 6A) and ubiquitination (Figure 6B) to the wild-type Twist1. Interestingly, mutation of the second motif on Twist1 S42A (Twist1 AVA) robustly stabilized Twist1 by blocking β-TrCP-mediated ubiquitination. These results suggest that T121 and S123 phosphorylation by AKT1 favor β-TrCP recognition for protein degradation likely due to a conformational change. We performed qChIP (Figure 6C) and luciferase assay (Figure 6D) to evaluate the transcriptional activities of the Twist1 variants on the E-cadherin promoter. While Twist1 S42A reduced its DNA binding ability and derepressed the transcriptional activity of the E-Cadherin promoter, additional mutation at T121 and S123 did not impact DNA binding or the transcriptional activity.

Functionally, we analyzed Twist1 variant-mediated EMT phenotype using retrovirus

infection in MCF7 cells. Interestingly, we found Twist1 S42A lost its EMT potential whereas Twist1 AVA induced EMT phenotypic change (Figure 6E) as well as cell invasion (Figure 6F). Together, our data indicated that AKT2/3 phosphorylates Twist1 at S42, reducing E-cadherin expression to induce EMT whereas AKT1 catalyzes extra two phosphorylation (T121 and S123) events on Twist1 for β-TrCP-mediated degradation to inhibit EMT (Figure 6G). Given most literature support that Twist1 does not directly and physically interact with the promoter, Twist1 42A likely changes the binding proteins complex to influence their DNA binding affinity.

**Correlation of AKT1, β-TrCP, Twist1, and E-cadherin in human tumor tissue**

To study AKT1-induced Twist degradation, we examined the protein expression of AKT1 and Twist1 in luminal and triple-negative breast cancer (TNBC) cell lines. Consistently, we observed significant downregulation of AKT1 and upregulation of Twist1 in TNBC cells (Figure 7A). Similar pattern was found when we compared triple-negative and luminal breast cancer patient samples (Figure 7B) in which AKT1 but not AKT2 correlated negatively with Twist1 in breast cancer patient samples (Figure 7C). Since downregulation of AKT1 induced tumor initiation cell population, we introduced non-stable knockdown of Twist1 in basal breast cancer cell lines and found a significant reduction of tumor initiating cells in most of the BLBC cell lines tested (Figure 7D). To further validate the pathological relevance of the identified mechanism, we studied the expression of AKT1, β-TrCP, Twist1, and E-cadherin in 104 human metastatic breast tumor specimens by immunohistochemical (IHC) staining. Twist1 was detected in 13 (12.6%) of the 39 specimens with high AKT1 expression but in 39 (37.9%) of the 45 specimens with low AKT1 expression, indicating that there is an inverse correction between AKT1 and Twist1 expression ($p$ = 0.018). Consistent with this finding, we found that AKT1

expression was associated with β-TrCP ($p$ = 0.0001) and E-cadherin expression ($p$ = 0.002) expression (Figures 7E and 7F). These IHC staining results further supported the pathological relevance of the identified pathway. Altogether, the results suggest that AKT1 phosphorylates multiple sites on Twist1 and that p-Twist1 reduces its DNA-binding activity to the E-cadherin promoter, which allows it to translocate to the cytoplasm where it recruits β-TrCP E3 ligase for ubiquitination and subsequently degradation. A proposed model for AKT1-mediated EMT suppression is illustrated in Figure 6G.

**Inhibition of AKT1 induces Twist1 upregulation and metastatic potential**

Multiple AKT inhibitors have been tested in clinical trials as anti-cancer agents (Pal et al., 2010). The model shown in Figure 6G raises a concern that the use of AKT inhibitors as anti-cancer agents could potentially enhance EMT/metastasis while suppressing tumor growth. To this end, we tested this potential adverse effect of a clinically used AKT inhibitor, MK-2206, which possesses differential inhibition toward AKT isoforms (selective inhibitor of AKT1, AKT2 and AKT3 with IC50 of 5 nM, 12 nM, 65 nM respectively) (Yap et al., 2011). To determine whether AKT1 inhibition by MK-2206 has potential to induce EMT via Twist1 upregulation in breast cancer cells, we treated MCF10A cells with 0.2 μM MK-2206 to measure the expression of EMT markers. We found that MK-2206 enhanced TGFβ-induced EMT (Figure 8A, lane 4, 8 and 12; and S7F). MK-2206 alone also induced EMT in MCF 10A cells but required a longer stimulation than TGFβ treatment (Figure 8A, lane 3, 7 and 11). Continuous treatment with MK-2206 alone to passage 3 (3 days/passage) led to late EMT morphological changes similar to that of TGFβ treatment. In fact, MK-2206-mediated EMT is primarily through AKT1 inhibition as knocking down AKT2 and AKT3 did not influence the EMT phenotype (Figure S7G). Consistent

with our earlier finding, inhibition of AKT1 by MK-2206 increases Twist1 stability by blocking Twist1 degradation (Figure 8A). To determine whether stabilization of Twist1 is required for MK-2006-mediated EMT, MCF 10A cells carrying shCTRL or shTwist1 (shTW-2) were treated with MK-2206 for 10 days. As shown in Figure 8B, downregulation of Twist1 inhibited MK2206-mediated cell migration, invasion, and formation of EMT phenotype, suggesting an indispensable role of Twist1 in MK-2206-mediated phenotypic changes associated with EMT.

Since the protein stability of Twist1 is tightly regulated by β-TrCP (Figure 4C and S5C), we asked whether destabilization of Twist1 by β-TrCP inducer resveratrol would reduce MK-2206-mediated EMT. To do this, we first treated MCF 10A cells with MK-2206 to induce EMT and then treated them with resveratrol (10 μM) for 2 days. We found that resveratrol downregulated Twist1 and reverted MK-2206-mediated phenotypic changes associated with EMT (Figure 8C). At a concentration of 10 μM, resveratrol inhibited MK-2206-mediated cell invasion (Figure 8D) and migration ability (Figure 8E). Similar experiments were also validated in MCF7 cells (Figures S7H, S7I and S7J). The possibility that resveratrol decreases the MK-2206-mediated aggressiveness was further explored by investigating the effects of resveratrol on tumor metastasis in animal model. To do this, 4T1 cells were transplanted into Balb/c mice via tail vein injections (Li et al., 2012). Tumor-bearing mice were then treated with or without MK-2206 or/and resveratrol. The metastatic nodules in the lungs were resected from each mouse and quantified by dissecting microscopy (Figure 8F). The number of lung metastasis was significantly reduced in mice co-treated with both MK-2206 and resveratrol but not in mice that received single regimen (Figure 8G). In addition, combination therapy of MK-2206 and resveratrol also prolonged mice survival by 20% (Figure 8H). These observations suggest that Twist1 is a key factor in MK-2206 induced EMT, cell migration/invasion, and lung colonization

in breast cancer and that destabilization of Twist1 enhances the therapeutic efficacy of MK-2206 for breast cancer treatment (Figure 8I). In fact, single regimen of MK-2206 was set to have 10%-20% efficacy to measure the combinatory effect. Therefore, MK-2206 treatment alone did not increase the number of metastatic lung nodules in Figures 8G.

**Discussion**

The discrepancies in AKT1's role in breast metastasis may be attributed to the differences in different transgenic models tested. While overexpression of AKT1 accelerated ErbB2-mediated mammary tumorigenesis but suppressed tumor invasion (Hutchinson et al., 2004), knockout of AKT1 in ErbB2 and PyMT in mice impaired lung metastasis (Ju et al., 2007; Maroulakou et al., 2007). Since knockout of AKT1 already compromised the ErbB2- and PyMT-induced primary tumor formation, it is unclear whether the reduced lung metastasis was attributed to the reduced primary tumor in that animal model. It should be noted that AKT1 was shown to induce EMT in squamous cancer and sacroma (Grille et al., 2003; Julien et al., 2007; Zhu et al., 2011). Here, we show that AKT1-mediated EMT inhibition was specifically found in breast cancer cells. Interestingly, this phenomenon was also correlated with the gene signature found in CCLE (Figure S1A). However, it remains unclear how AKT1 activity is modulated within different cell context. In this study, we find that AKT1 expression is negatively correlated with EMT phenotype by cross-analysis of available datasets from both cell lines and patient samples. We show that AKT1 interacts with Twist1 and reverses its transcriptional repression function in E-cadherin regulation. Three Ser/Thr residues spanning two AKT phosphorylation motifs of Twist1 are required for its complete phosphorylation by AKT1 *in vitro* and *in vivo*. Twist1 mutant that is no longer phosphorylated by AKT1 fails to be ubiquitinated by β-TrCP for subsequent degradation, resulting in the acquisition of EMT aggressiveness. This mechanism predicts and

prompts us to report an adverse effect of MK-2206 therapy in inducing metastatic potential in breast cancer cells.

Activation of the PI3K-AKT pathway has been shown to involve in the negative feedback regulation of S6K, mTOR, MEK, and RTK (O'Reilly et al., 2006; Sridharan and Basu, 2011; Turke et al., 2012). The combined therapy by blocking AKT activity has shown promising outcome compared to single regimen. However, AKT-mediated negative feedback loop is less understood. To date, AKT inhibition relieves feedback suppression of HER3 expression and activation in breast cancer cells (Chandarlapaty et al., 2011). AKT also downregulates insulin-like growth factor-1 receptor as a result of a negative feedback mechanism (Qin et al., 2011). We now show that AKT1 phosphorylates Twist1 to induce its degradation as a potential negative feedback regulation to inhibit metastasis. Consistently, we observed a strong correlation between AKT1 and Twist1 downregulation in metastatic breast cancer cohorts (Figure 6). Together, these results indicate that enabling this feedback regulation by AKT1 inhibition in breast cancer patients is likely to induce Twist1 upregulation which subsequently promotes metastasis.

The involvement of Twist1 in PI3K/AKT signaling was first identified using a nonbiased approach in which both Twist1 and AKT2 were found to be elevated in highly invasive stable cell lines (Cheng et al., 2007). Vichalkovski et al. previously showed that AKT2/PKBβ phosphorylates Twist1 at S42 and S123 in an *in vitro* system (Vichalkovski et al., 2010) However, site-specific phospho-antibodies did not reveal the S123 phosphorylation site *in vivo*, suggesting that S42 is the predominant site responsible for AKT2-induced phosphorylation in some cell types (Vichalkovski et al., 2010). Aside from an earlier study showing PKAU phosphorylates Twist1 S123, our results indicate that Twist1 S42, T121, and S123 are all exclusively phosphorylated by AKT1 *in vitro* and *in vivo*. Mutation of any of these three sites did

not disrupt or only partially disrupted of Twist1 phosphorylation by AKT1, suggesting that these two motifs can compensate for the loss of one or the other. It is noteworthy to mention that AKT1 and AKT2 share similar but not identical phosphorylation activities (Zhang et al., 2006), which may contribute to their differential downstream effects (Zhou et al., 2006) (Kato et al., 2007) (Wani et al., 2011). Interestingly, knockdown or overexpression of AKT2 had no effect on Twist1 stability (Figure 3C, 3D and 3F).

Functionally, phosphorylation at S42 by AKT2 has been shown to be essential for the anti-apoptosis activity of Twist1, and ablation of S42 phosphorylation sensitized cells to adriamycin-induced apoptosis (Vichalkovski et al., 2010). Since Twist1 is an EMT regulator and is phosphorylated by AKT1, our investigation with the Twist1 AVA mutant reveals a negative role of AKT1 in cell migration, invasion, and EMT (Figure 5A-C, S7A and S7B), resembling the negative role of AKT1 during metastasis (Dillon and Muller, 2010). We reason that phosphorylation occurs at different cellular stages within different contexts, and therefore, could give rise to a distinct functionality. It is also likely that the affinity of Twist1 to the E-cadherin promoter is lowered due to the conformational change in the bHLH motif which requires the phosphorylation of S42. Although this study focuses on EMT suppression mediated by AKT1 but not AKT2, the cellular compartmentalization of AKT subtypes is an important yet challenging factor in studying their distinct functions (Gonzalez and McGraw, 2009).

It is worthwhile to mention that p-S42 is detected only in cancer tissues and correlated with high levels of p-AKT (Xue et al., 2012). We reasoned that the correlation between Twist1 p-S42 and p-AKT is likely due to high intrinsic AKT2/3 expression in the invasive patient cohorts. Because AKT1 mediates Twist1 degradation through additional phosphorylation at T121 and S123, the staining of high levels of p-S42 is likely attributed to AKT2/3. As illustrated in

Supplementary Figure S7K, due to the significant downregulation of AKT1 during breast cancer metastasis, the effect of AKT2 and AKT3 on Twist1 exceeded that of AKT1 in invasive patient samples.

We found that not only DN-AKT1 (Figure 5E) but also inhibition of AKT1 kinase activity by MK-2206 (Figure 8A) was able to induce EMT in breast cancer cells, which suggests that the involvement of AKT1 in the EMT inhibition is kinase dependent. To determine the putative AKT1 substrate among the EMT regulators, we compared their interactions with AKT1 (Figure S2E) and the presence of phospho-motif (Figure 4A) and determined that Twist1 is an authentic AKT1 substrate that is directly involved in AKT1-mediated EMT inhibition. As the GSK3β and Snail axis is often related to AKTs signaling, AKT1 may counteract EMT inhibition by repressing GSK3β/Snail signaling. In this study, we provided several lines of evidence to exclude the possible involvement of Snail by AKT1 in breast cancer cells: 1) AKT1 did not directly interact with or phosphorylate Snail (Figure 2F, S2E and S3D); 2) only Twist1 but not Snail was upregulated in shAKT1-induced EMT cells in breast cancer cells (Figure 3B and 3C); and 3) only Twist1 but not Snail was upregulated in AKT1 inhibitor MK2206-induced EMT cells (Figure 8A). These results indicate that the myr-AKT1-mediated GSK3β activation is not sufficient to induce Snail stabilization in breast cancer cells (Figure 3B) and suggest that it may be worthwhile to revisit the specific function of AKT1, 2 or 3 in different cell types.

Because AKT does not influence Twist1 mRNA expression (Vichalkovski et al., 2010) (data not shown) and Twist1 undergoes caspase-mediated cleavage and proteasome-mediated degradation (Demontis et al., 2006), it is reasonable to investigate the protein stability of Twist1 in response to AKT1 activation. In agreement with an earlier report that AKT1 but not AKT2 targets S-phase kinase-associated protein 2 for degradation (Lin et al., 2009), we identified the

isoform-specific, phosphorylation-dependent degradation of Twist1. In fact, studies with regard to AKT-mediated proteasome degradation are prevalent. For example, PI3K/AKT has been shown to destabilize p53 (Ogawara et al., 2002), FOXO3a (Brunet et al., 1999), and Bax (Datta et al., 1997) to block their negative regulatory functions, thereby promoting cell growth and survival. Aside from rapid degradation of the tumor suppressors, AKT also maintains the homeostatic stability of a wide variety of oncoproteins via phosphorylation-dependent degradation. By cooperating with MDM2, AKT induces proteasome-mediated degradation of androgen receptor in prostate cells (Lin et al., 2002). AKT also reverses overexpression of TAL1 in leukemic cells by inducing proteolysis for the proper maintenance of intracellular concentrations of TAL1 (Terme et al., 2009). Similar to our earlier observations in GSK3β-mediated Snail destabilization in EMT repression (Zhou et al., 2004), AKT1 also serves as a critical signaling factor in regulating Twist1 stability.

Since β-TrCP is a novel E3 ligase targeting AKT1-Twist1 complexes for degradation, we tested the effect of resveratrol (3,5,4'-trihydroxystilbene), which is currently being studied in clinical trials (www.clinicaltrials.gov), on β-TrCP induction to limit the metastatic potential induced by MK-2206. Resveratrol is a naturally occurring compound that has been investigated for its beneficial effects in diet and cancer progression. Except for its anti-tumorigenesis activity, a number of studies have indicated that resveratrol functions in anti-metastasis through induction of β-TrCP expression (Wei et al., 2009; Wei et al., 2007). In particular, our data provide a mechanism by which resveratrol inhibits MK-2206-induced breast cancer metastasis through the Twist1/β-TrCP degradation pathway. Since inhibition of AKT1 relieves its suppression on Twist1 and results in EMT, the use of resveratrol as an inhibitor of anti-AKT1-triggered EMT has the potential to reverse this effect. Although both shAKT and AKT1-DN increased lung colonization

(Figure 5F and 5I) and MK-2206 enhanced EMT ability (Figure 8A-E), MK-2206 alone did not increase lung colonization (Figure 8G) in the model established via intravenous injection of 4T1 cells. Because the experiment was set to test combinatory effect, MK-2206 mediated AKT1 inhibition in mice treatment was not optimized. In addition, the cytotoxicity of MK-2206 may suppress the survival of tumor cells after intravenous injection. The number of cells required for lung colonization after MK-2206 treatment may not be sufficient compared to untreated cells.

While down regulation of AKT1 in mesenchyme/BLBC cells is promising, the dramatic expression of AKT3 throughout most cancer cells (Figure S1B) suggests that isoform-specific p-AKT3 antibody has the potential to serve as a biomarker to indicate triple-negative status of breast tumor tissues. In regard to its high expression in mesenchyme or TNBC cells (Figure 1A, 1B, 1C, and 1D), specific small molecule inhibitor against AKT3 may eliminate the isoform effect of AKT1. Given the effective treatment for TNBC remains unavailable, AKT3 may be tested as a therapeutic target for TNBC.

In summary, we have identified a novel AKT1/β-TrCP/Twist1/E-cadherin signaling axis in breast cancer cells (Figure 7E). The AKT1- and AKT2/3-specific EMT regulation of Twist1 phosphorylation appear to have differential effects depending on the cellular context. Dissecting the effect of each AKT isoform, in this case, AKT1 enabled us to further understand how breast cancer cells undergo EMT and reach metastatic potential. Moreover, perturbation of this pathway by resveratrol may be beneficial by limiting the metastatic potential when administering MK-2206.

## EXPERIMENTAL PROCEDURES

*Cell lines and cell culture*. All cell lines were obtained from the American Type Culture

Collection (Manassas, VA) and maintained in Dulbecco's modified Eagle's medium containing high glucose (DMEM/F-12) with 10% fetal bovine serum (FBS). Stable cell lines were grown in the presence of an additional 500 mg/ml G418 (Invitrogen, Carlsbad, CA) or 1 μg/ml puromycin (Calbiochem, San Diego, CA).

*Immunohistochemical (IHC) Staining.* IHC staining was performed as described previously (Lee et al., 2007). Human breast tumor tissue specimens were incubated with antibodies against AKT1, β-TrCP, Twist1 or E-cadherin and a biotin-conjugated secondary antibody and then incubated with an avidin-biotin-peroxidase complex. Visualization was performed using amino-ethylcarbazole chromogen. For statistical analysis, Fisher's exact test and Spearman rank correlation coefficient were used and a p-value less than 0.05 is considered statistically significant.

*Mouse Model of Lung Metastasis.* Tumor metastasis assays were performed using an intravenous breast cancer mouse model as previous described (Li et al., 2012). 4T1 Cells ($1 \times 10^5$) were injected into the lateral tail vein of Balb/c mice. To measure lung metastases, animals were weighed before each experimental end point, and lung nodules were stained with India ink, excised, and counted immediately. All animal works were performed in accordance with MD Anderson institutional review board and was performed in accordance with National Institutes of Health guideline. Detailed treatment protocol is described in Supplemental Information.

All other experimental procedures are described in the Supplemental Information.

**Acknowledgments**

We would like to thank Markeda L. Wade at Scientific Publication at MD Anderson Cancer Center for editing the manuscript. We thank Dr. Bryant G. Darnay in the Department of Experimental Therapeutics at MD Anderson Cancer Center for providing the pMX-Flag retrovirus virus expression system. This work was partially supported by the National Institutes of Health (R01 CA109311 and PO1 CA099031), Susan G. Komen, Patel Memorial Breast Cancer Endowment Fund, National Breast Cancer Foundation, National Institutes of Health Breast Cancer SPORE (CA116199) and Cancer Center Support Grant (CA16672); Breast Cancer Research Foundation grant (to M.-C.H. and G.N.H.), The University of Texas MD Anderson-China Medical University and Hospital Sister Institution Fund (to M.-C. Hung), Cancer Research Center of Excellence (DOH102-TD-C-111-005, Taiwan), Program for Stem Cell and Regenerative Medicine Frontier Research (NSC101-2321-B-039-001, Taiwan), International Research-Intensive Centers of Excellence in Taiwan (NSC102-2911-I-002-303, Taiwan), Center for Biological Pathways, and U.S. Army Breast Cancer Research Program Postdoctoral Fellowship (W81XXWH-10-1-0598; to C.-W.L.).

# Figure 1

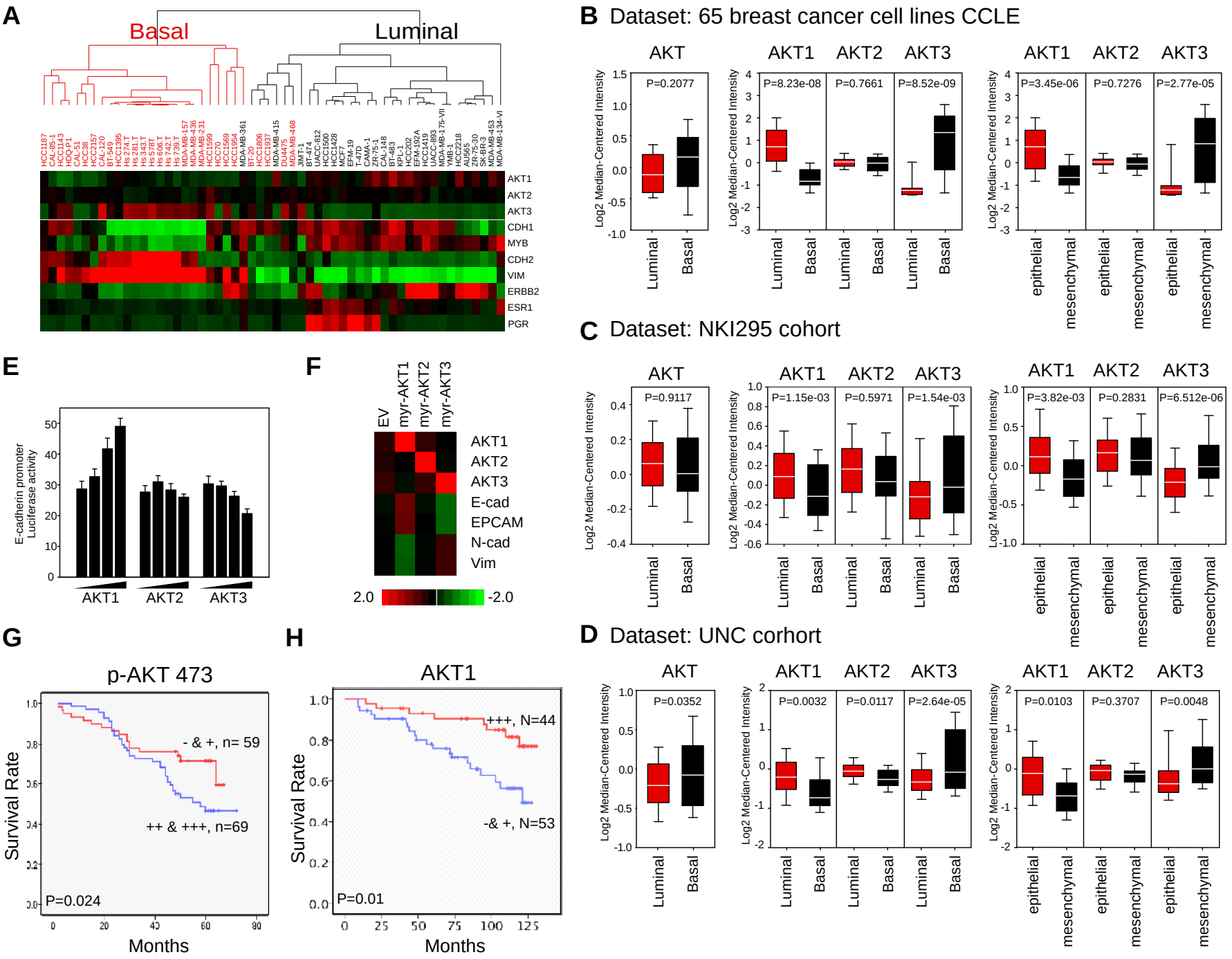
A
Basal
Luminal
AKT1
AKT2
AKT3
CDH1
MYB
CDH2
VIM
ERBB2
ESR1
PGR
B Dataset: 65 breast cancer cell lines CCLE
AKT
AKT1 AKT2 AKT3
Log2 Median-Centered Intensity
P=0.2077
P=8.23e-08
P=0.7661
P=8.52e-09
P=3.45e-06
P=0.7276
P=2.77e-05
Luminal
Basal
epithelial
mesenchymal
C Dataset: NKI295 cohort
P=0.9117
P=1.15e-03
P=0.5971
P=1.54e-03
P=3.82e-03
P=0.2831
P=6.512e-06
D Dataset: UNC corhort
P=0.0352
P=0.0032
P=0.0117
P=2.64e-05
P=0.0103
P=0.3707
P=0.0048
E
E-cadherin promoter Luciferase activity
AKT1
AKT2
AKT3
F
EV
myr-AKT1
myr-AKT2
myr-AKT3
AKT1
AKT2
AKT3
E-cad
EPCAM
N-cad
Vim
2.0
-2.0
G
p-AKT 473
Survival Rate
- & +, n= 59
++ & +++, n=69
P=0.024
Months
H
AKT1
+++, N=44
-& +, N=53
P=0.01
Months

# Figure 2

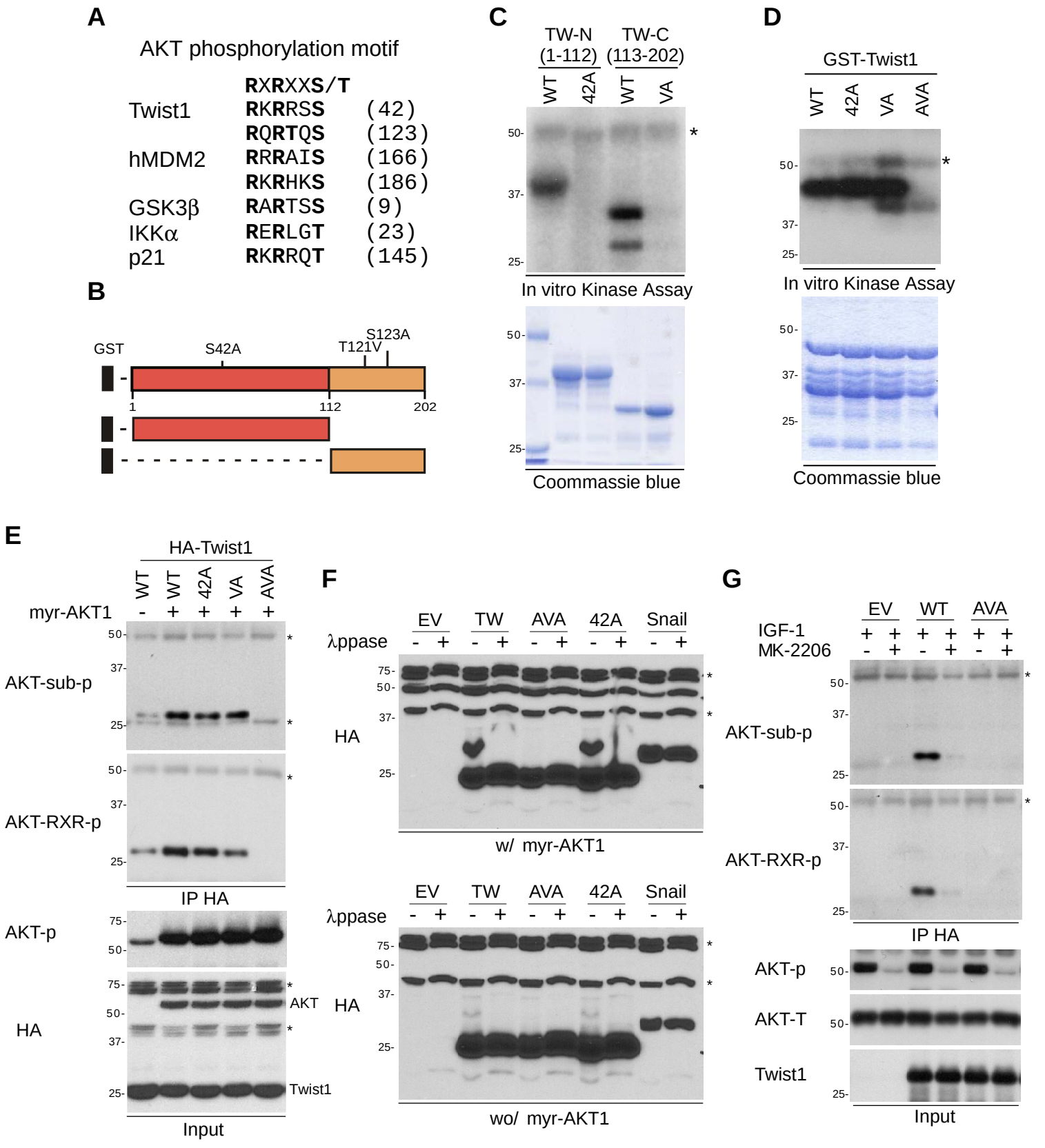
A
AKT phosphorylation motif
RXRXXS/T
Twist1 RKRRSS (42)
RQRTQS (123)
hMDM2 RRRAIS (166)
RKRHKS (186)
GSK3β RARTSS (9)
IKKα RERLGT (23)
p21 RKRRQT (145)
B
GST
S42A
S123A
T121V
1
112
202
C
TW-N (1-112)
TW-C (113-202)
WT
42A
WT
VA
50-
37-
25-
In vitro Kinase Assay
Coommassie blue
D
GST-Twist1
WT
42A
VA
AVA
In vitro Kinase Assay
Coommassie blue
E
HA-Twist1
WT
WT
42A
VA
AVA
myr-AKT1 - + + + +
AKT-sub-p
AKT-RXR-p
IP HA
AKT-p
HA
AKT
Twist1
Input
F
EV
TW
AVA
42A
Snail
λppase - + - + - + - + - +
HA
w/ myr-AKT1
wo/ myr-AKT1
G
EV
WT
AVA
IGF-1 + + + + + +
MK-2206 - + - + - +
AKT-sub-p
AKT-RXR-p
IP HA
AKT-p
AKT-T
Twist1
Input

# Figure 3

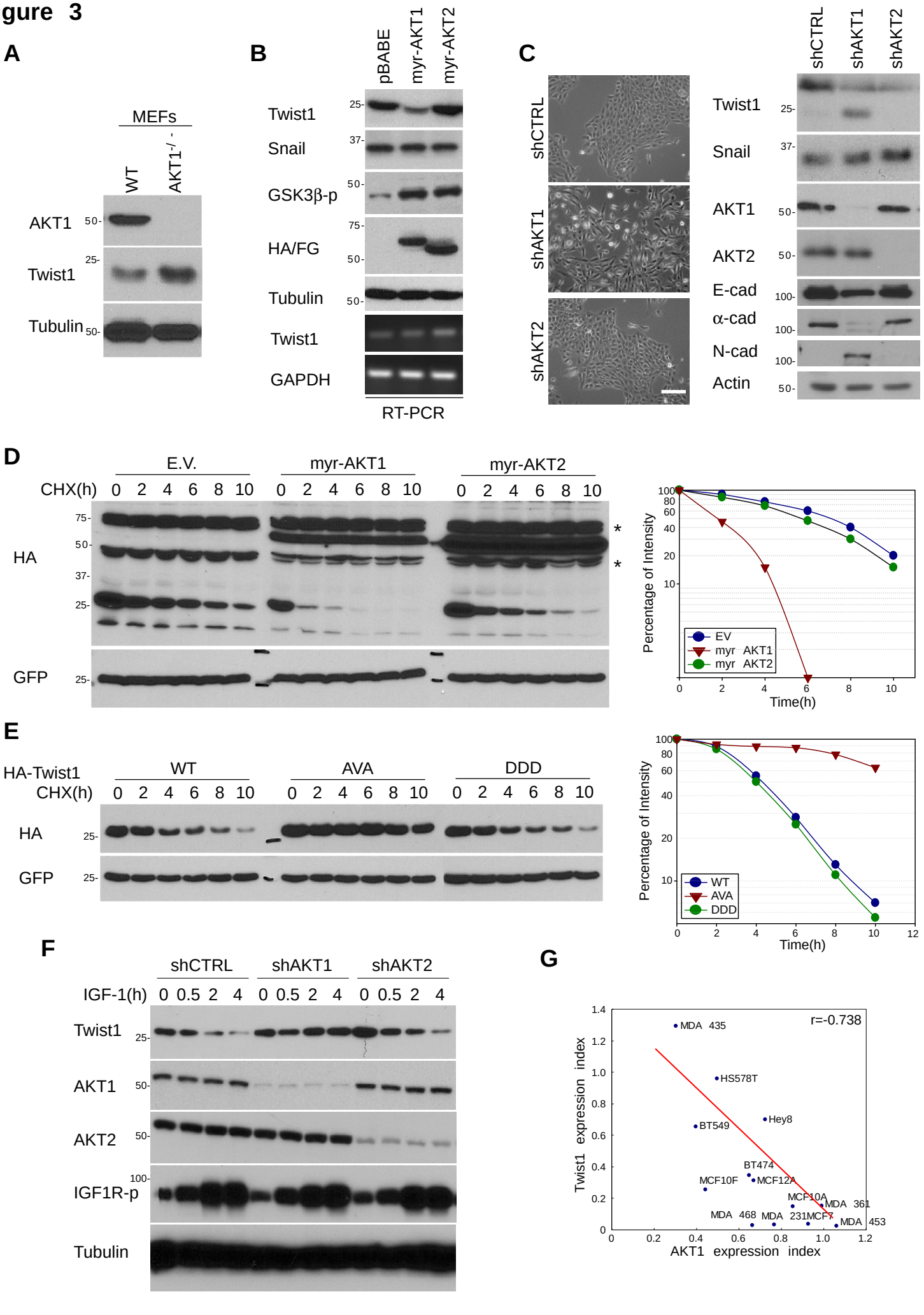
A
MEFs
WT
AKT1-/-
AKT1
Twist1
Tubulin
B
pBABE
myr-AKT1
myr-AKT2
Twist1
Snail
GSK3β-p
HA/FG
Tubulin
Twist1
GAPDH
RT-PCR
C
shCTRL
shAKT1
shAKT2
Twist1
Snail
AKT1
AKT2
E-cad
α-cad
N-cad
Actin
D
E.V.
myr-AKT1
myr-AKT2
CHX(h) 0 2 4 6 8 10
HA
GFP
Percentage of Intensity
Time(h)
EV
myr AKT1
myr AKT2
E
HA-Twist1
WT
AVA
DDD
CHX(h) 0 2 4 6 8 10
HA
GFP
Percentage of Intensity
Time(h)
WT
AVA
DDD
F
shCTRL
shAKT1
shAKT2
IGF-1(h) 0 0.5 2 4
Twist1
AKT1
AKT2
IGF1R-p
Tubulin
G
r=-0.738
MDA 435
HS578T
Hey8
BT549
BT474
MCF10F
MCF12A
MCF10A
MDA 361
MDA 468
MDA 231
MCF7
MDA 453
Twist1 expression index
AKT1 expression index

# Figure 4

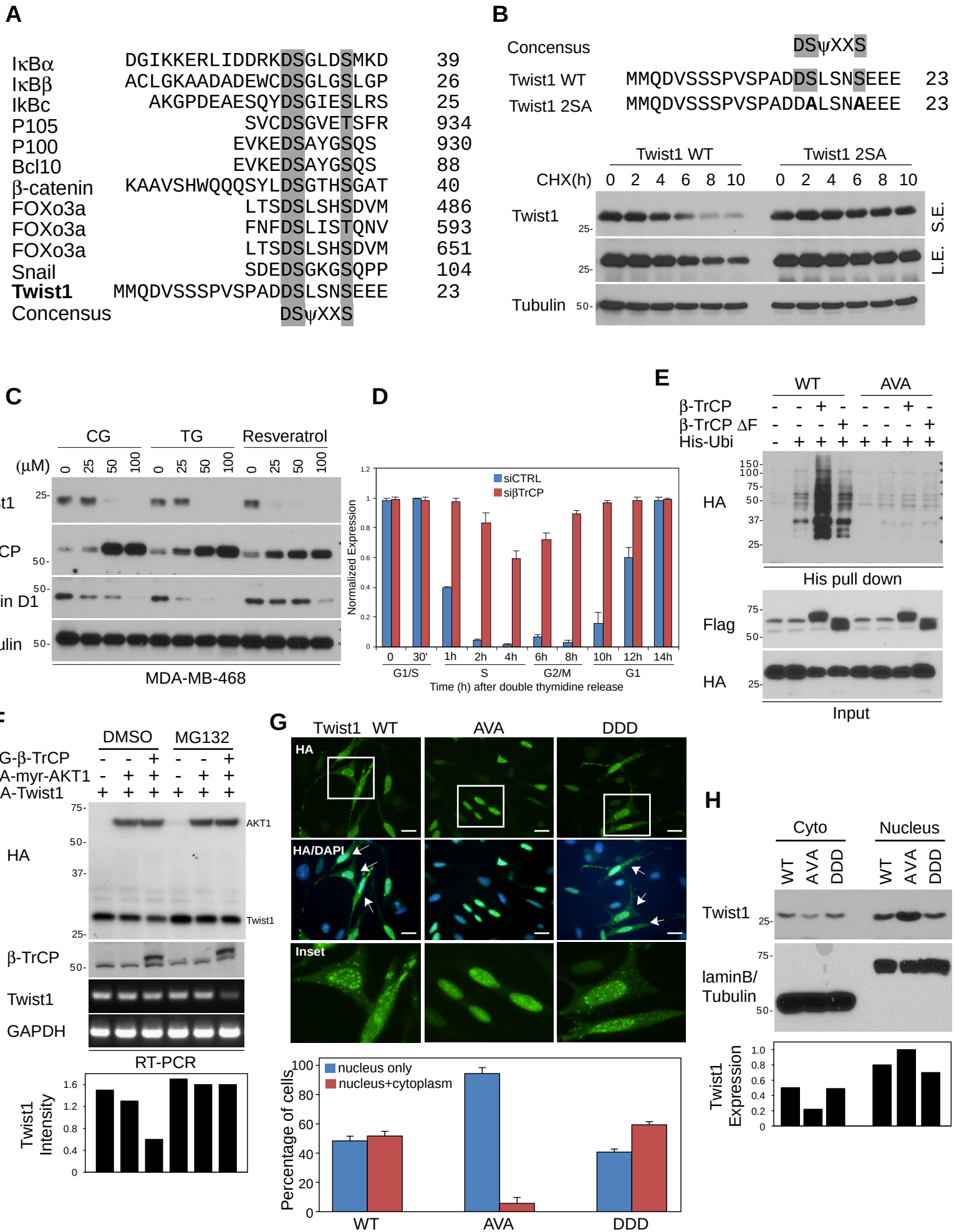
A
IκBα DGIKKERLIDDRKDSGLDSMKD 39
IκBβ ACLGKAADADEWCDSGLGSLGP 26
IkBc AKGPDEAESQYDSGIESLRS 25
P105 SVCDSGVETSFR 934
P100 EVKEDSAYGSQS 930
Bcl10 EVKEDSAYGSQS 88
β-catenin KAAVSHWQQQSYLDSGTHSGAT 40
FOXo3a LTSDSLSHSDVM 486
FOXo3a FNFDSLISTQNV 593
FOXo3a LTSDSLSHSDVM 651
Snail SDEDSGKGSQPP 104
Twist1 MMQDVSSSPVSPADDSLSNSEEE 23
Concensus DSψXXS
B
Concensus DSψXXS
Twist1 WT MMQDVSSSPVSPADDSLSNSEEE 23
Twist1 2SA MMQDVSSSPVSPADDALSNAEEE 23
Twist1 WT
Twist1 2SA
CHX(h) 0 2 4 6 8 10 0 2 4 6 8 10
Twist1
Tubulin
S.E.
L.E.
C
CG
TG
Resveratrol
(μM) 0 25 50 100 0 25 50 100 0 25 50 100
Twist1
β-TrCP
Cyclin D1
Tubulin
MDA-MB-468
D
siCTRL
siβTrCP
Normalized Expression
0 30' 1h 2h 4h 6h 8h 10h 12h 14h
G1/S S G2/M G1
Time (h) after double thymidine release
E
WT AVA
β-TrCP
β-TrCP ΔF
His-Ubi
HA
His pull down
Flag
HA
Input
F
DMSO MG132
FG-β-TrCP
HA-myr-AKT1
HA-Twist1
HA
AKT1
Twist1
β-TrCP
Twist1
GAPDH
RT-PCR
Twist1 Intensity
G
Twist1 WT AVA DDD
HA
HA/DAPI
Inset
nucleus only
nucleus+cytoplasm
Percentage of cells
WT AVA DDD
H
Cyto Nucleus
WT AVA DDD WT AVA DDD
Twist1
laminB/ Tubulin
Twist1 Expression

# Figure 5

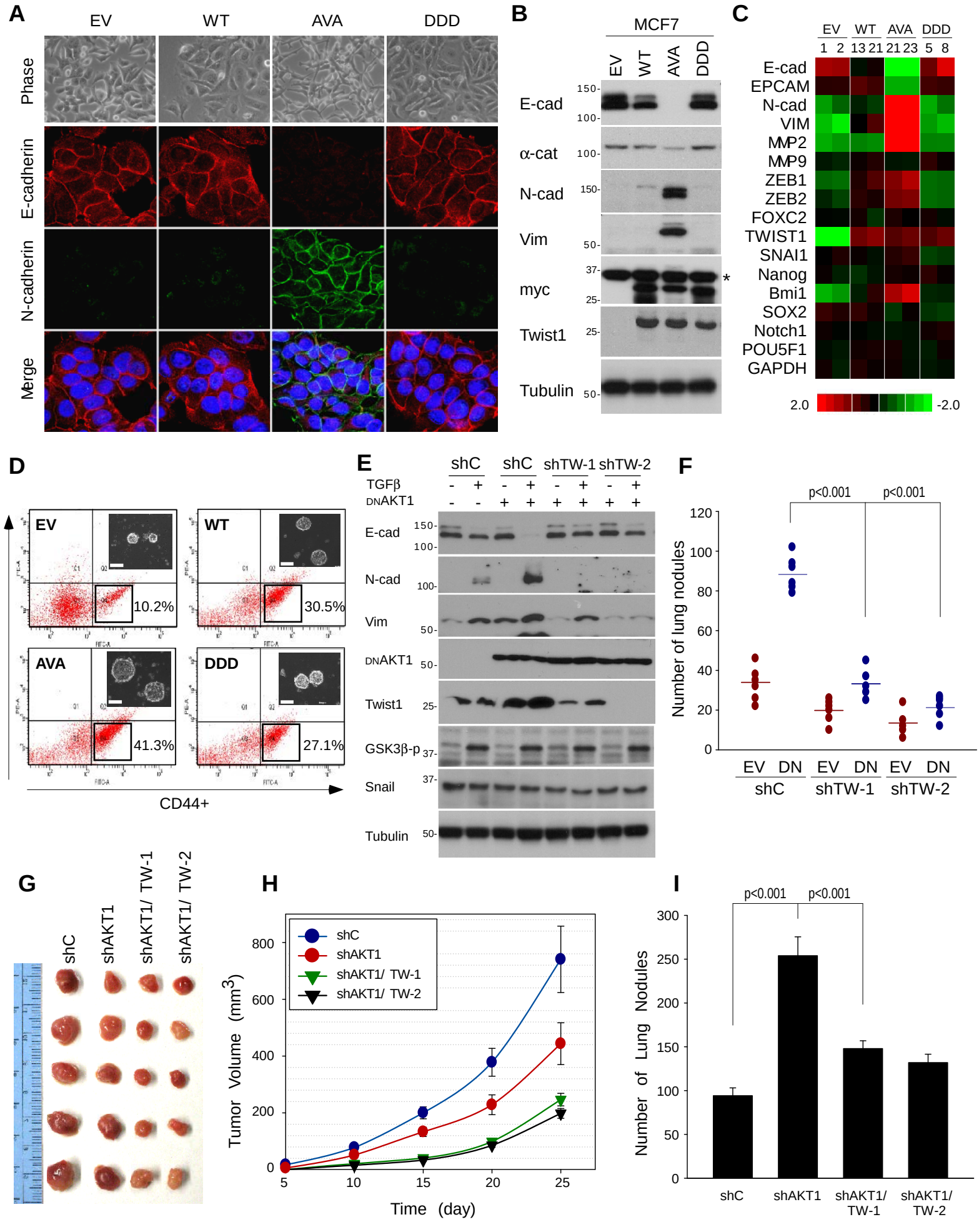
A
EV
WT
AVA
DDD
Phase
E-cadherin
N-cadherin
Merge
B
MCF7
EV
WT
AVA
DDD
E-cad
α-cat
N-cad
Vim
myc
Twist1
Tubulin
150-
100-
50-
37-
25-
*
C
EV
WT
AVA
DDD
1 2 13 21 21 23 5 8
E-cad
EPCAM
N-cad
VIM
MMP2
MMP9
ZEB1
ZEB2
FOXC2
TWIST1
SNAI1
Nanog
Bmi1
SOX2
Notch1
POU5F1
GAPDH
2.0
-2.0
D
EV
WT
AVA
DDD
10.2%
30.5%
41.3%
27.1%
CD24-
CD44+
E
shC
shC
shTW-1
shTW-2
TGFβ
DNAKT1
E-cad
N-cad
Vim
DNAKT1
Twist1
GSK3β-p
Snail
Tubulin
150-
100-
50-
37-
25-
F
p<0.001
p<0.001
Number of lung nodules
120
100
80
60
40
20
0
EV DN EV DN EV DN
shC shTW-1 shTW-2
G
shC
shAKT1
shAKT1/ TW-1
shAKT1/ TW-2
H
shC
shAKT1
shAKT1/ TW-1
shAKT1/ TW-2
Tumor Volume (mm3)
800
600
400
200
0
5 10 15 20 25
Time (day)
I
p<0.001
p<0.001
Number of Lung Nodules
300
250
200
150
100
50
0
shC
shAKT1
shAKT1/ TW-1
shAKT1/ TW-2

# Figure 6

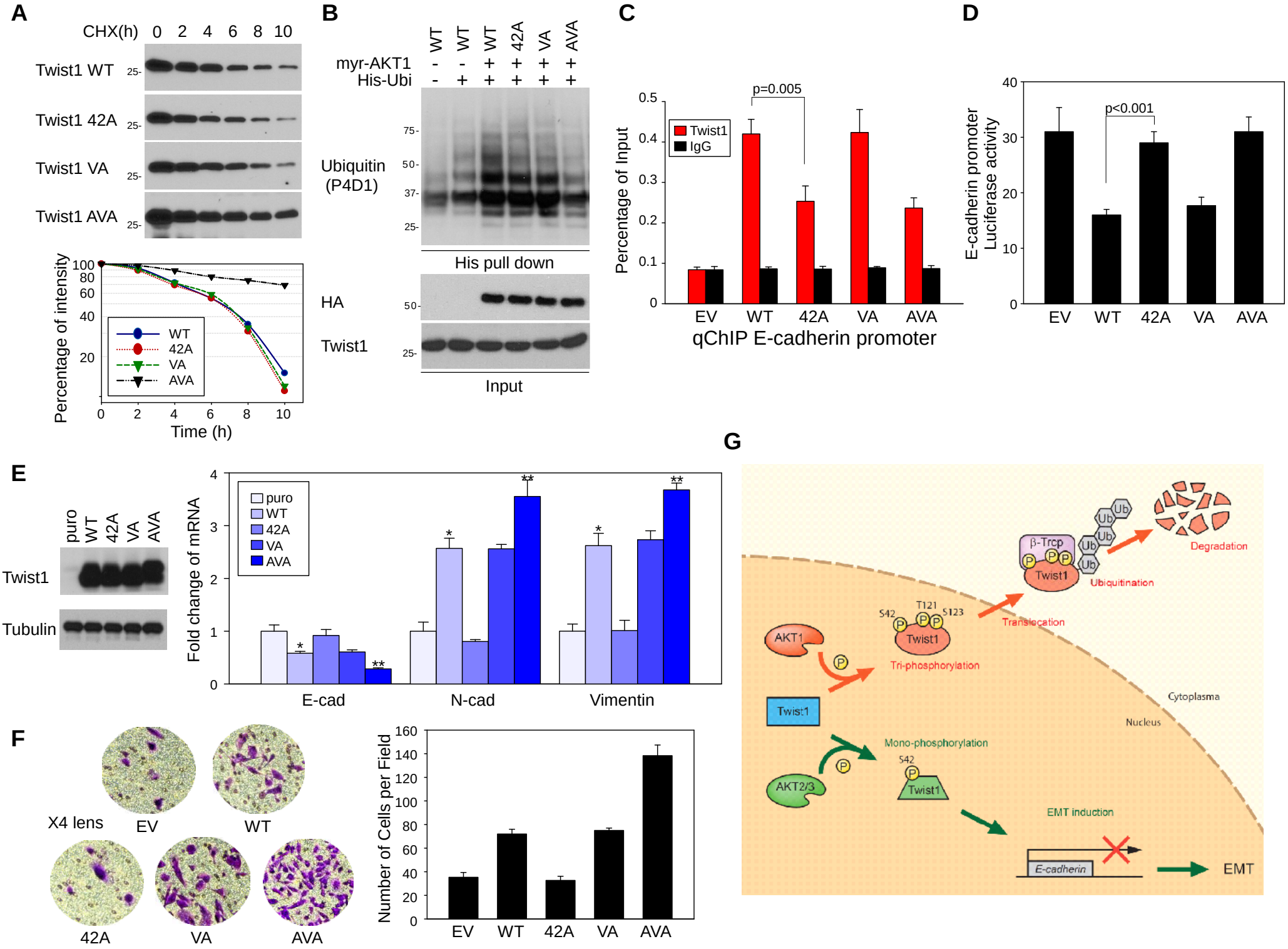
A
CHX(h) 0 2 4 6 8 10
Twist1 WT
Twist1 42A
Twist1 VA
Twist1 AVA
25-
Percentage of intensity
100
80
60
40
20
WT
42A
VA
AVA
0 2 4 6 8 10
Time (h)
B
WT WT WT 42A VA AVA
myr-AKT1 - - + + + +
His-Ubi - + + + + +
Ubiquitin (P4D1)
75-
50-
37-
25-
His pull down
HA
Twist1
50-
25-
Input
C
Percentage of Input
0.5
0.4
0.3
0.2
0.1
0
p=0.005
Twist1
IgG
EV WT 42A VA AVA
qChIP E-cadherin promoter
D
E-cadherin promoter Luciferase activity
40
30
20
10
0
p<0.001
EV WT 42A VA AVA
E
puro WT 42A VA AVA
Twist1
Tubulin
Fold change of mRNA
4
3
2
1
0
puro
WT
42A
VA
AVA
*
**
E-cad N-cad Vimentin
F
X4 lens
EV
WT
42A
VA
AVA
Number of Cells per Field
160
140
120
100
80
60
40
20
0
EV WT 42A VA AVA
G
β-Trcp
Ub
Degradation
Twist1
Ubiquitination
Translocation
S42
T121
S123
AKT1
Tri-phosphorylation
Cytoplasma
Nucleus
Mono-phosphorylation
AKT2/3
EMT induction
E-cadherin
EMT

# Figure 7

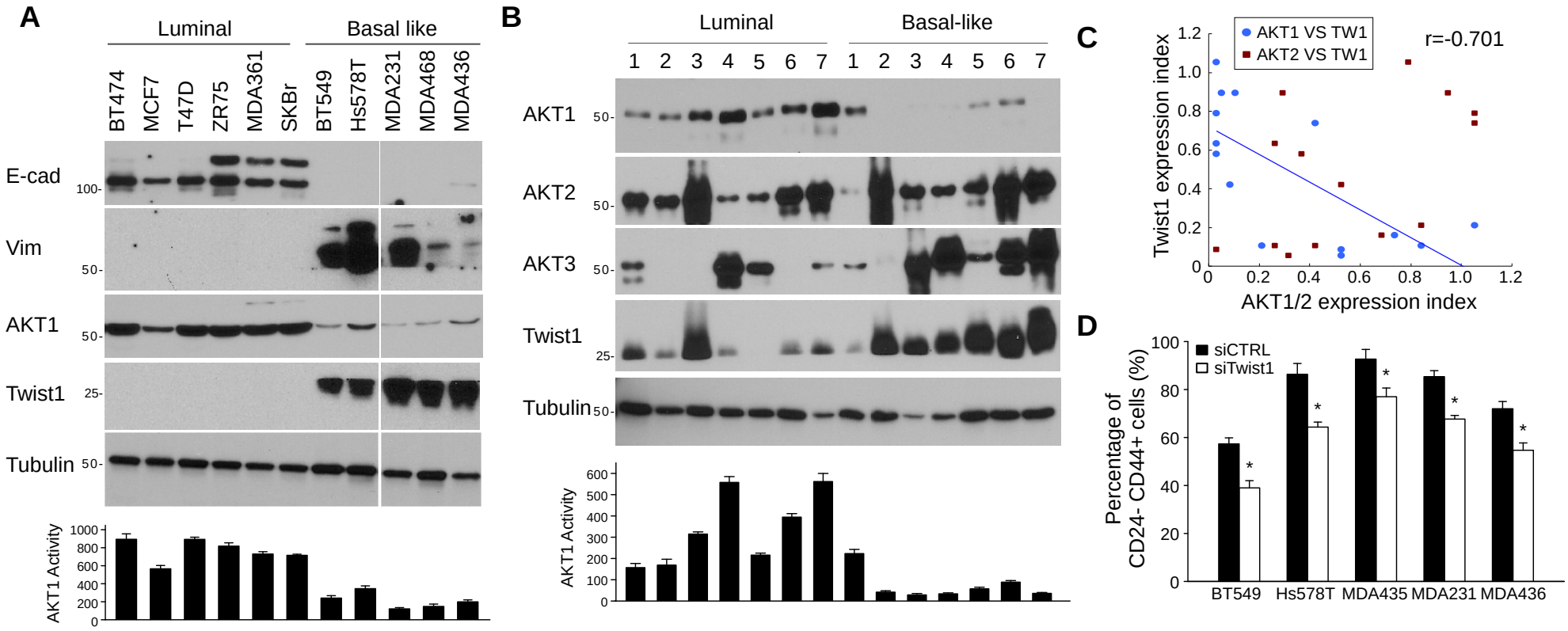


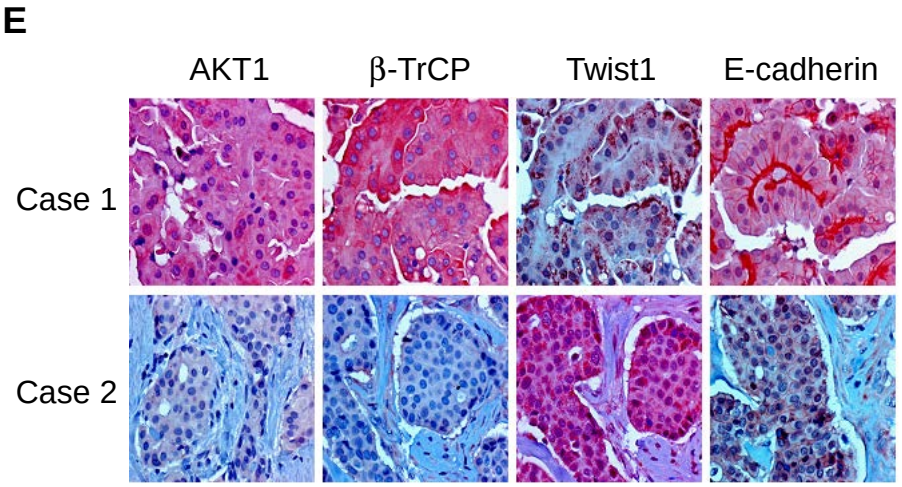


F

| | | AKT1 Expression | | | | |
|---|---|---|---|---|---|---|
| | | - / + | ++ | +++ | Total | p value |
| β-TrCP | -/+ | 15(14.4%) | 8(7.7%) | 1(1.0%) | 24(23.1 % | |
| | ++ | 7(6.7%) | 17(16.3%) | 5(4.8%) | 29(27.9 )% | |
| | +++ | 1(1.0%) | 8(7.7%) | 42(40.4%) | 51(49.0 )% | |
| Total | | 23(22.1 %) | 33(31.7%) | 48(46.2%) | 104 (100)%) | P= 0.0001 |
| Twist1 | -/+ | 6(5.8%) | 9(8.7%) | 13(12.6%) | 28(27.2%) | |
| | ++ | 21(20. 4%) | 3(2.9%) | 17(16.5%) | 41(39.8%) | |
| | +++ | 18(17.5%) | 7(6.8%) | 9(8.7%) | 34(33.0%) | |
| Total | | 45(43.7%) | 19(18.4%) | 39(37.9%) | 103(100%) | P=0.018 |
| E-Cad | -/+ | 12(14.5%) | 7(8.4%) | 3(3.6%) | 22(26.5 % | |
| | ++ | 5(6.0%) | 9(10.8%) | 14(16.9%) | 28 (33.7 )% | |
| | +++ | 4(4.8%) | 10(12%) | 19(22.9%) | 33 (39.8)% | |
| Total | | 21(25.3%) | 26(31.3 %) | 36(43.4 %) | 83(100%) | P= 0.002 |

# Figure 8

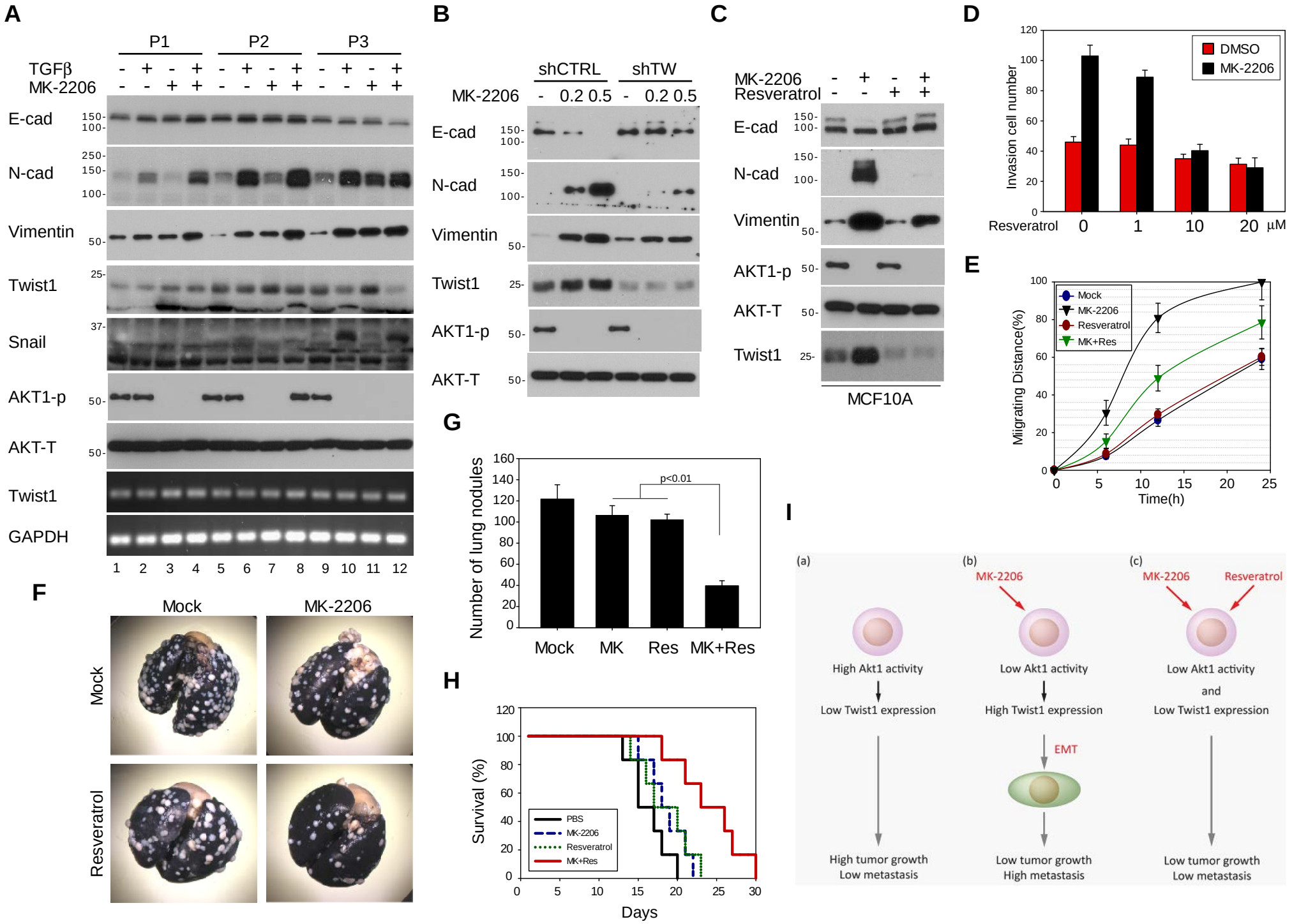
A
P1
P2
P3
TGFβ
MK-2206
E-cad
N-cad
Vimentin
Twist1
Snail
AKT1-p
AKT-T
Twist1
GAPDH
1 2 3 4 5 6 7 8 9 10 11 12
B
shCTRL
shTW
MK-2206 - 0.2 0.5 - 0.2 0.5
E-cad
N-cad
Vimentin
Twist1
AKT1-p
AKT-T
C
MK-2206
Resveratrol
E-cad
N-cad
Vimentin
AKT1-p
AKT-T
Twist1
MCF10A
D
DMSO
MK-2206
Invasion cell number
Resveratrol 0 1 10 20 μM
E
Mock
MK-2206
Resveratrol
MK+Res
Migrating Distance(%)
Time(h)
F
Mock
MK-2206
Mock
Resveratrol
G
Number of lung nodules
p<0.01
Mock MK Res MK+Res
H
Survival (%)
PBS
MK-2206
Resveratrol
MK+Res
Days
I
(a)
(b)
(c)
MK-2206
Resveratrol
High Akt1 activity
Low Twist1 expression
High tumor growth
Low metastasis
Low Akt1 activity
High Twist1 expression
EMT
Low tumor growth
High metastasis
Low Akt1 activity
and
Low Twist1 expression
Low tumor growth
Low metastasis